Transportation Research Part B 121 (2019) 216–251

Contents lists available at ScienceDirect

Transportation Research Part B

journal homepage: www.elsevier.com/locate/trb

Optimization of traffic sensor location for complete link flow observability in traffic network considering sensor failure

Mostafa Salari[a], Lina Kattan[a,*], William H.K. Lam[b], H.P. Lo[b], Mohammad Ansari Esfeh[a]

[a] Department of Civil and Environmental Engineering, Schulich School of Engineering, University of Calgary, Calgary, Alberta, Canada
[b] Department of Civil and Environmental Engineering, The Hong Kong Polytechnic University, Hung Hom, Kowloon, Hong Kong, China

ARTICLE INFO

Article history:
Received 7 August 2018
Revised 14 January 2019
Accepted 15 January 2019
Available online 6 February 2019

Keywords:
Network sensor location problem
Full link flow observability
Partial observability
Flow observation
Route flow information
Sensor failure
Redundant sensors
Genetic algorithm

ABSTRACT

The full link flow observability problem is to identify the minimum set of traffic sensors to be installed in links in a road traffic network. The sensors are used to both monitor the flow of observed links and to provide flow information for the link flow inference of unobserved links. Unavoidably, the traffic sensors deployed in a traffic network are subject to failure which leads to missing the link flow observation of observed links as well as the inability to infer the link flow of unobserved links. This study aims to identify the minimum set of links in a traffic network to be instrumented with two different types of counting sensors (basic and advanced sensors) to reach full link flow observability while minimizing the effect of sensor failure on the link flow inference of unobserved links. Mathematically, we formulate two objective functions including min-max and min-sum functions. The first function attempts to minimize the maximum effect of sensor failure on the link flow inference of unobserved links while the second one minimizes the expected number of unobserved links where flow cannot be inferred due to the failure of sensors. We select the genetic algorithm (GA) as a well-known heuristic to solve the proposed optimization model. The results recommend minimizing the number of sensors required for the link flow inference of each unobserved link as well as installing advanced sensors on links involved in the link flow inference of multiple unobserved links. We also develop a new objective function to reflect that links in a traffic network can be either minor or major roads with different levels of importance. The results suggest installing more advanced sensors on the major roads as well as minimizing the number of major roads included in the set of unobserved links. Concerning the availability of route flow information in a network, we consider the effect of this information on evaluating the sensor deployment in a network. To maintain full link flow observability of a traffic network if any sensor fails, we study the location and type of additional sensors introduced as redundant sensors, which are more than the minimum required for full link flow observability. Finally, we discuss the applicability of the proposed model for the partial observability problem in which the full link flow observability conditions are not satisfied.

* Corresponding author.
E-mail address: lkattan@ucalgary.ca (L. Kattan).

https://doi.org/10.1016/j.trb.2019.01.004

1. Introduction

1.1. Background and motivation

Identifying the location of sensors in a traffic network, known as the network sensor location problem, is a critical component of transportation network modeling. Sensors provide essential information on the trip distribution and the corresponding spatiotemporal characteristics of traffic patterns in traffic zones in vehicular networks. However, the reliability and quality of information provided by sensors is highly dependent on the failure rate of sensors (Zhu et al., 2017). According to historical records, the failure rate of counting sensors[1] exceeds 25% for all types of sensor deployments (Federal Highway Administration, 2006), yet the repair cost of these sensors may be too high for traffic agencies considering their limited budgets (Danczyk et al., 2016). Moreover, information loss is another consequence of sensor failure that imposes an implicit cost to a traffic management system.

For a fully observable traffic network, the flow of all links can be either directly observed (i.e., flow of observed links by sensors) or indirectly inferred (i.e., flow of unobserved links, based on information obtained from the flow of observed links). The failure of sensors not only impedes observing the flow of observed links, but also results in missing link flow information associated with unobserved links since the flows of these links are inferred using the link flow information obtained from observed links. However, the sensor configuration can effectively mitigate the adverse effect of sensor failure on information loss in a network. Therefore, there is an urgent need for a sensor configuration that minimizes the effect of sensor failure as a source of uncertainty in current traffic management applications.

The current literature in the traffic flow observability/estimation problem identifies the three most important sources of uncertainty associated with traffic flow data as (1) the variability of prior Origin-Destination (OD) demand; (2) measurement errors of traffic counts; and (3) the possibility of missing the flow information due to the failure of sensors (Danczyk et al., 2016). The variability of prior OD demand is mainly related to the flow estimation problem as it deals with the reliability of information required to be used for traffic flow estimation. For instance, Fei et al. (2007) and Fei and Mahmassani (2011) employed the Kalman filtering technique to find the sensor locations that maximize information gains through the observed data and minimize the errors of estimated OD demands. Zhou and List (2010) optimized the locations of automatic vehicle identification (AVI) sensors by maximizing the gain of observed information in an uncertain environment. Wang et al. (2012) minimized the variance in the posterior route flow estimation while considering the available information on route flows and the reliability of this information. In a similar study, Wang and Mirchandani (2013) addressed the optimum locations of sensors based on the reliability of prior route flow information. Sensor measurement error, as another source of uncertainty, has been studied in recent published works related to the flow observability problem. For instance, Castillo et al. (2010) addressed the scanning errors while locating vehicle identification (Vehicle-ID) sensors in a traffic network. More recently, Xu et al. (2016) discussed the full link flow observability problem and proposed a robust approach that determines the links to be equipped with sensors in a traffic network regarding the flow measurement variance stemmed from sensors.

To the best of our knowledge, the failure of sensors has received less attention in flow observability/estimation research, with the exception of two studies (Li and Ouyang, 2011; Danczyk et al., 2016). Li and Ouyang (2011) examined the location of vehicle-ID sensors in a network to maximize the information gain from OD routes considering the possibility of sensor failure, while Danczyk et al. (2016) addressed the installation of counting sensors on a freeway to minimize the overall freeway performance monitoring errors resulting from the failure of sensors. However, the consideration of sensor failure on the link flow observation/inference of links in a fully observable network is absent in current studies related to the flow observability problem.

Our work attempts to fill a void in the literature by making the following main contributions: First, to reach full link flow observability, we develop a new mathematical optimization model for optimizing sensor configuration that considers the probability of sensor failure. Second, we incorporate the possibility of installing non-identical sensors, with different failure probabilities and costs, on links with different levels of importance in a network. We also consider the effect of high heavy vehicle loads (HVL) on failure probability of sensors and the corresponding sensor positioning in a network. Third, with respect to the availability of route flow information, we discuss the loss of this information due to the failure of sensors and add a new consideration for sensor positioning evaluation. Fourth, based on the suggested layout of sensors, we propose a new approach for locating redundant sensors in a traffic network to minimize the effect of sensor failure on the full link flow observability. Finally, to address economic impediments to reach full link flow observability, we evaluate the effectiveness of the proposed model for partial link observability in a network.

Before proceeding, a formal definition of the terminology used in this paper is provided below:

Observed and unobserved links: If a link is equipped with a sensor, then that link is named an observed link; otherwise it is an unobserved link.

Link flow observation and link flow inference: If the flow of a link is monitored by a sensor installed on that link then the flow of that link will be observed. This process is called *link flow observation*. On the other hand, if the flow of a link is

[1] For the remainder of the paper, “counting sensors” are called “sensors”.

inferred, using the link flow information obtained from observed links, it is then called *link flow inference*. In summary, the process of link flow observation and link flow inference occur for observed links and unobserved links, respectively.

Missing link flow inference: Link flow inference of an unobserved link will be missed if the failure occurs for at least one of the sensors installed on the observed link(s) required for the link flow inference of that unobserved link.

The remainder of this paper is organized as follows: The rest of this section reviews the existing literature on the flow observability problem. Sections 2 and 3 discuss the motivating example and the link flow inference. Section 4 addresses the effect of failure in link flow inference. Sections 5–7 explain the model formulation, the effect of route flow information on evaluating sensor locations, and redundant sensors, respectively. Sections 8 and 9 discuss the solution algorithm and the case studies. Finally, the applicability of the proposed model for partial observability problem and the conclusion are provided in Sections 10 and 11, respectively.

1.2. Classification of the flow observability problem

In the literature, Gentili and Mirchandani (2012) classified the network sensor location problem into two categories: (i) the sensor location flow estimation problem and (ii) the sensor location flow observability problem. The sensor location flow estimation problem concerns finding the optimum location of sensors to minimize traffic flow estimation errors, while the sensor location flow observability problem attempts to determine the location that requires the least number of sensors to make full or partial traffic flow observability possible. The solutions obtained in the flow observability problem are mainly based on network topological information, i.e., information on links connectivity and enumeration of routes. However, the flow estimation problem usually requires additional information, including the historical traffic flows in a network, since this type of problem attempts to use this historical information to estimate current traffic flow data. The readers may refer to Chootinan et al. (2005), Chen et al. (2007), Ehlert et al. (2006), Gentili and Mirchandani (2018), Hadavi and Shafahi (2016), and Zhan et al. (2018) for a further review of the literature related to the sensor location flow estimation problem.

The sensor location flow observability problem includes studies that attempt to maximize/minimize the objective functions related to traffic flow observations. As an example of a multi-objective problem, Viti et al. (2014) addressed the observability problem to maximize the traffic flow information gain obtained from sensors and to minimize the number of sensors to be located on links. There are also some studies which attempt to satisfy one or more predetermined objectives, known as goal-oriented problems. In one such study, Yang and Bell (1998) defined a mathematical model that determines the number of sensors to be located on nodes to observe a given fraction of the traffic flow. In a more recent work, Fu et al. (2017) used matrix arithmetic to obtain the full link observability as the goal of their model in the presence of the link-path incidence matrix.

Many of the studies which addressed the flow observability problem cannot be assigned to either category, as they usually mix multi-objective and goal-oriented problems to simultaneously pursue several aims, as well as to meet some predefined goals often defined as constraints in their formulations. As a way of illustration, He (2013), Hu et al. (2009), Ng (2012), and Xu et al. (2016) investigated the minimum number of sensors that should be installed on links with the assumption of no prior information (i.e., information on turning ratio at an intersection, link choice proportions, and the route choice behavior of users) to observe or infer the flow of all links in a traffic network. For instance, Hu et al. (2009) employed an algebraic approach to identify the location of sensors on links for full link flow observability assuming the existence of the link-path incidence matrix to represent a network. In another work, He (2013) used the topological tree characteristics of solutions to determine the minimum set of links to be equipped with sensors for the full link observability.

The sensor location flow observability problem can also be categorized according to traffic flow observation types. Based on the classification introduced by Castillo et al. (2013), there are four types of observability problems: link flow observability, OD flow observability, route flow observability and general case flow observability.

(1) *Link flow observability*: In this category, the aim is to determine which subset of links or nodes should be instrumented with sensors to enable link flow inference of unobserved links. The link flow observability problem itself can be divided into two subproblems concerning the location of sensors, which can either be on nodes (Bianco et al., 2001, 2006; Morrison and Martonosi, 2015) or on links (Bianco et al., 2014; Hu et al., 2009; Ng, 2012, 2013; Xu et al., 2016). Both of these subproblems deal with a linear system of equations and attempt to obtain the unknown values related to unobserved link flows using independent equations.

(2) *OD flow observability*: Observing the ongoing flow between each OD pair is the purpose of OD flow observability problem. The OD flow information can be obtained counting link flows or route flows (See Castillo et al., 2008a; Mínguez et al., 2010). It is possible that the OD flow observability using link flow information has infinite solutions, known as the under-specified problem. To overcome under-specification, some researchers suggest using additional information including the prior information of OD-pair flows and network properties (Castillo et al., 2008b).

(3) *Route flow observability*: In relatively large networks, there is usually more than one path or route between each OD pair. Obtaining information about the flow of each route is the goal of route flow observability problem. Route flow knowledge can also provide OD flow and link flow information by using flow conservation equations. Studies addressing the route flow observability problem can be classified based on the types of sensors employed in their target network. For instance, some studies attempt to obtain route flow information using counting sensors (Hu et al., 2009; Rinaldi and Viti, 2017) while others use different techniques and types of sensors to acquire this information.

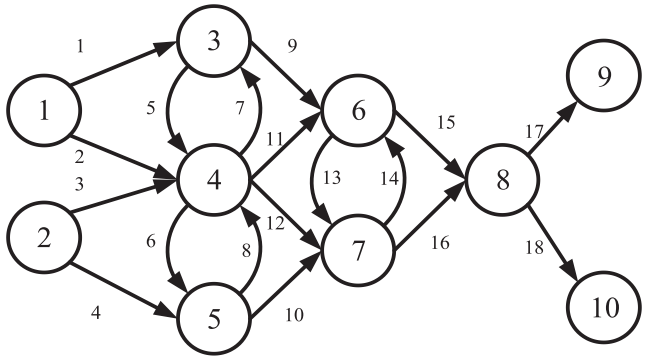

Fig. 1. Fishbone network.

For instance, plate scanning techniques which give information about the flow of a route or part of a route using license plate recognition (LPR) sensors is an alternative to the link counts technique (Castillo et al., 2013).

(4) *General case flow observability*: This case happens when the flow of interest is not limited to one of the three categories described above. In fact, the goal of general flow observability could be to observe the flow of links, routes and OD flows simultaneously (Castillo et al., 2010; Fei et al., 2013). For instance, Castillo et al. (2010) developed a matrix tool for general observability in traffic networks.

Castillo et al. (2013) introduced the *link flow observability problem* as the simplest one among other observability problems. Although, recently, there have been many more studies addressing the link flow observability problem in the literature. This trend is due to the fact that this type of observability problem requires the least prior information of a traffic network while other types of problems depend on additional information which might not be available for large-scale networks. For instance, information about the number of OD pairs and the number of paths in a network must be available to solve *OD flow observability* or *route flow observability* problems, respectively. However, as the size of a traffic network increases, it becomes more challenging to obtain these pieces of information (Ng, 2012). Another reason for the current focus on the *link flow observability problem* is that most of the studies addressing the flow observability problem are designed to be employed for the strategic planning of a traffic network (Xu et al., 2016). Since it is difficult for urban planners to obtain the prior information required for other types of observability problems at the planning stage, planners prefer to rely on the least amount of prior data.

2. Motivating example

Consider the example of the Fishbone network which was first introduced by Hu et al. (2009). This network has 18 directed links and four centroid nodes, i.e., nodes 1 and 2 as origin nodes and nodes 9 and 10 as destination nodes (See Fig. 1). The other nodes, including nodes 3, 4, 5, 6, 7, and 8, are non-centroid nodes.

According to Ng (2012), to reach the full link flow observability in a network, we need to equip a minimum of $(\frac{(|J|-|I|)}{|J|}) \times 100$ percent of links with sensors, where J and I represents the set of links and non-centroid nodes in a network, respectively.[2] This means that at least 66.67% of the links, i.e., 12 links, of the Fishbone network should be equipped with sensors to make this network fully observable. Note that the flow of the other six links, i.e., unobserved links, can be inferred using the link flow information of observed links, i.e., sensor-equipped links, while according to Ng (2012), different sets of links can be considered as the set of observed links in a network. The layouts introduced in Fig. 2 are two of the many possible layouts to reach full link flow observability in the Fishbone network.

According to Fig. 2, there are six unobserved links as well as 12 observed links in each of layouts A and B. Fig. 2 also introduces the linear system of equations required to infer the flow of unobserved links in each layout using the link flow information of observed links. Sensors installed in observed links similar to any other measurement apparatus are subject to failure and their failure can affect the link flow inference of unobserved links. This means that in an equation existing in either of the linear systems introduced in Fig. 2, the flow of an unobserved link cannot be inferred if at least one of the sensors installed on the observed links in that equation breaks down. Considering the failure probability of sensors located on the observed links, we can calculate the probability of missing/not inferring the link flow of unobserved links.

For instance, the probability of missing the link flow inference of the unobserved link 4 in layouts A and B is determined in Table 1.

In Table 1, p is the failure probability of a sensor and it is assumed all sensors are identical having the same probability of failure and functioning independently. According to the last column of Table 1, the unobserved links which need a smaller

[2] To determine the minimum number of links to be equipped with sensors, Ng (2012) specifies an upper bound for the set of all possible links whose flow can be inferred to reach full link flow observability in a network.

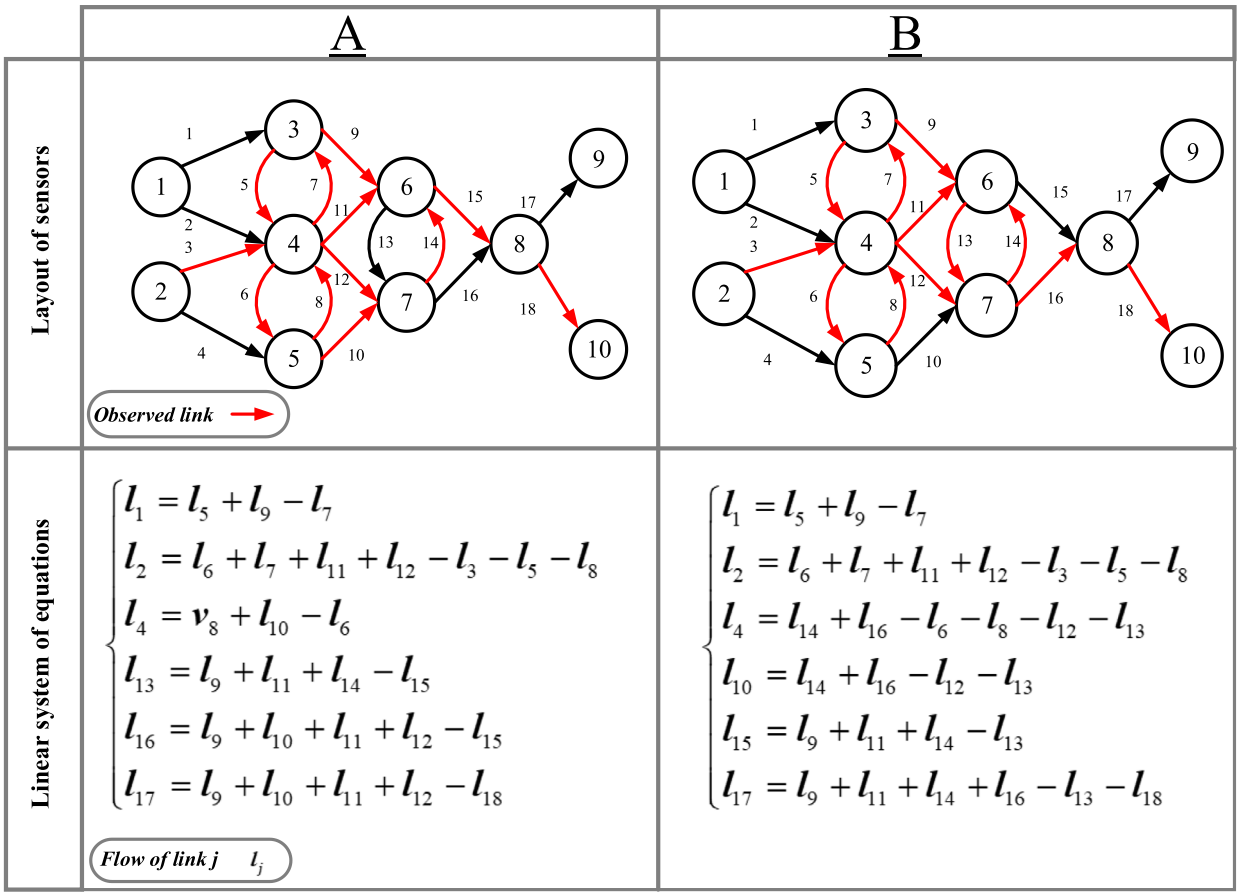

Fig. 2. Two possible layouts to reach full link flow observability in Fishbone network.

Table 1
Probability of missing the link flow inference of the unobserved link 4.

Layout	Link flow inference equation	Possibility of missing the link flow inference (Identical sensors)
A	$l_4 = l_8 + l_{10} - l_6$	$1-(1-p)^3$
B	$l_4 = l_{14} + l_{16} - l_6 - l_8 - l_{12} - l_{13}$	$1-(1-p)^6$

Table 2
Failure effect of the sensor installed on link 9 in layouts A and B.

Layout	Equations including link 9	Set of unobserved links requiring link 9	Expected number of unobserved links (Identical sensors)
A	$l_1 = l_5 + l_9 - l_7$ $l_{13} = l_9 + l_{11} + l_{14} - l_{15}$ $l_{16} = l_9 + l_{10} + l_{11} + l_{12} - l_{15}$ $l_{17} = l_9 + l_{10} + l_{11} + l_{12} - l_{18}$	{1, 13, 16, 17}	$4p$
B	$l_1 = l_5 + l_9 - l_7$ $l_{15} = l_9 + l_{11} + l_{14} - l_{13}$ $l_{17} = l_9 + l_{11} + l_{14} + l_{16} - l_{13} - l_{18}$	{1, 15, 17}	$3p$

number of observed links for their link flow inference tend to have a lower chance of missing their link flow inference due to the failure of sensors. For instance, the chance of missing the link flow inference of unobserved link 4 in layout A is lower than the chance of missing the link flow inference of the same link in layout B. Therefore, a possible layout that requires fewer observed links for the link flow inference of each unobserved link is a preferred layout assuming all sensors are identical.

Until now, we have only considered the *probability* of missing link flow inference for a given set of unobserved links. In addition, we are also interested in exploring the *effect* of a sensor's failure on the link flow inference of unobserved links. For instance, we compare the failure effect of the sensor installed on observed link 9 in layouts A and B (See Table 2).

According to Table 2, the observed link 9 appears in four different equations of the linear system related to layout A while this observed link exists in three different equations of the linear system related to layout B. This means that the flow of 4 unobserved links (links 1, 13, 16 and 17) in layout A cannot be inferred if the sensor installed on link 9 breaks down. However, the flow of only three unobserved links (links 1, 15, and 17) cannot be inferred if the sensor installed on link 9 in layout B stops functioning. Considering the failure probability of the sensor installed on link 9, we can also find the expected number of unobserved links for which flow cannot be inferred due to the failure of the sensor located on link 9 in each layout. The last column of Table 2 represents this expected value assuming that the sensors installed on link 9 in both layouts A and B are identical. According to this column, the lower the number of appearances of an observed link in different equations required for the link flow inference of unobserved links, the lower the expected number of unobserved links for which flow cannot be inferred due to the failure of the sensor installed on that observed link.

In Tables 1 and 2, we assumed that the sensors are identical, each having similar failure probability. In this study, we are also interested in examining the possibility of installing different types of sensors, i.e., non-identical sensors, with dissimilar failure probability. The probability of missing the link flow inference of unobserved links due to the failure of identical or non-identical sensors, as well as the effect of each sensor failure on the link flow inference of unobserved links, motivated us to determine the location of sensors in a network to minimize the adverse effect of sensor failure.

3. Link flow inference: locating sensors on links

Inferring link flows based on the traffic flow information of links instrumented with sensors is referred to as the link flow inference. Node-based and route-based methods are two main techniques to infer link flows. Node-based approaches use the flow conservation rule for non-centroid nodes to infer link flows, while route-based methods are based on link-path incidence equations. Ng (2012) suggested the use of a node-based approach to avoid the path enumeration problem. Therefore, in this work, we also employ this approach to infer link flows. The flow conservation rule for a set of links connected to a node can be shown as follows:

$$\sum_{j\in In(i)} l_j - \sum_{j\in Out(i)} l_j + BF_i = 0 \tag{1}$$

where l_j represents the ongoing flow on the link j. $In(i)$, $Out(i)$ and BF_i are the set of links with a head at node i, a tail at node i, and the balancing flow at node i, respectively. For a non-centroid node, the BF should be equal to zero. Therefore, for each non-centroid node, the above equation changes to Eq. (2).

$$\sum_{j\in In(i)} l_j - \sum_{j\in Out(i)} l_j = 0 \qquad \forall i \in I \tag{2}$$

For a traffic network consisting of $|I|$ non-centroid nodes and $|J|$ links, Eq. (2) can be written as the following system of linear equations:

$$T_{|I|\times|J|}L_{|J|\times 1} = 0 \rightarrow \begin{cases} t_{11}l_1 + t_{12}l_2 + \ldots + t_{1|J|}l_{|J|} = 0 \\ t_{21}l_1 + t_{22}l_2 + \ldots + t_{2|J|}l_{|J|} = 0 \\ . \\ . \\ . \\ t_{|I|1}l_1 + t_{|I|2}l_2 + \ldots + t_{|I||J|}l_{|J|} = 0 \end{cases} \tag{3}$$

where T is the node-link incidence matrix, which is defined for non-centroid nodes. For this linear system, t_{ij} is equal to $+1$ if j is an incoming link to node i. Otherwise, if j is an outgoing link from node i, then t_{ij} equals -1, and it equals 0 if j is neither an incoming nor an outgoing link to/from node i. The number of non-centroid nodes, $|I|$, and the number of links, $|J|$, respectively comprise the number of equations and variables of this system. A linear system has a unique solution when the number of equations equals the number of unknown variables and all equations are linearly independent. Thus, in the linear system of Eq. (3), we can determine the value of a maximum number of $|I|$ unknown variables when the remainder variables, $|J| - |I|$, are known, and all $|I|$ equations of this system are independent. The flow conservation rule using a node-based approach for a traffic network can also be written as follows (Ng, 2012):

$$\underbrace{\begin{pmatrix} T_u & T_o \end{pmatrix}}_{T} \underbrace{\begin{pmatrix} l_u \\ l_o \end{pmatrix}}_{L} = 0 \tag{4}$$

where T_o and T_u are the sub-matrices of T relating to observed and unobserved links, respectively. The linear system of Eq. (4) can also be shown as follows:

$$T_u l_u + T_o l_o = 0 \Rightarrow l_u = -{T_u}^{-1} T_o l_o \tag{5}$$

According to Eq. (5), the node-link matrix corresponding to unobserved links, T_u, should be an invertible matrix with the rank of $|I|$ to make it possible to infer the flow of unobserved links, l_u, while according to Ng (2012), the matrix T_u is not necessarily unique. In what follows, we introduce one of the methods for constructing the matrix of unobserved links.

Table 3
Set of links for the Fishbone network.

Non-centroid node	Connected links	Set of new links to nodes
3	1,5,7,9	{1, 5, 7, 9}
4	2,3,5,6,7,8,11,12	{2, 3, 6, 8, 11, 12}
5	4,6,8,10	{4, 10}
6	9,11,13,14,15	{13, 14, 15}
7	10,12,13,14,16	{16}
8	15,16,17,18	{17, 18}

3.1. The concept of new links

Initially introduced by Castillo et al. (2014), the *new link* method is further developed by Xu et al. (2016) as a means to build the matrix of unobserved links. According to this method, each link assigned to a set of new links related to a non-centroid node should be a link connected to that node and shouldn't already be assigned to other sets of new links. In other words, the set of new links associated with a non-centroid node include *all links* connected to that node excluding the links which are already allocated to other sets of new links. To create the sets of new links, we usually start from the first non-centroid node and continue constructing these sets for all other non-centroid nodes. It is possible that some sets of new links become empty sets in a network, as the links connected to those nodes are already assigned to the sets of new links associated with other non-centroid nodes. The following equations show the rules to be followed in constructing the set of new links:

$$J = \bigcup_{i \in I} H_i \tag{6}$$

$$H_i \cap H_{i'} = \varnothing \qquad \forall i, i' \in I \tag{7}$$

where J and I are the set of links and non-centroid nodes in a network, respectively. H_i and $H_{i'}$ represent the set of new links assigned to the non-centroid nodes i and i'. According to Eq. (6), the union of all sets of new links should be equal to the set of links. Moreover, Eq. (7) guarantees that there is no intersection between any set of new links in a network. As a way of illustration, Table 3 shows the set of new links for the network depicted in Fig. 1.

The second column of Table 3 shows the links connected to each non-centroid node in the node-link incidence matrix belonging to the network in Fig. 1. The last column of this table shows the sets of *new links* assigned to each non-centroid node. As can be seen for each set, the link(s) allocated to a non-centroid node are not assigned to any other non-centroid node. Xu et al. (2016) proposed that "*the maximum set of unobserved links to be inferred from observed links can be found by selecting any single new link assigned to each non-centroid node*".[3] Note that the term "*maximum*" indicates that depending on the topology of a network, the number of sets of new links can be less than the number of non-centroid nodes (i.e., some sets of new links associated with non-centroid nodes become empty sets). The links selected from each non-empty set of new links are then used to create the matrix of unobserved links, i.e., T_u, while the structure of sets of new links prevents the selected links from inducing a cyclic graph and becoming a non-invertible matrix.

4. The effect of sensor failure on the link flow inference of unobserved links

In this section, we investigate the importance of sensor failure in determining the set of observed links in a network to reach full link flow observability. To do so, we explore the objective function(s) required to minimize the effect of sensor failure on the link flow inference of unobserved links. According to the motivating example, two contributing factors in determining the set of observed links, considering the failure of sensors, include the probability of missing the link flow inference of unobserved links as well as the effect of sensor failure on the link flow inference of unobserved links. We further discuss these two factors with respect to situations in which the sensors are identical or not. The probability of failure of identical sensors is assumed to be the same regardless of their cost and their employed technology. This assumption can be beneficial when there are not enough historical records about the failure of different type of sensors. However, if this information is available, we can develop a more specific model considering non-identical sensors having different probabilities of failure. Note that in both scenarios, we assume that the sensors are installed independently and there is no correlation between the failure of any pair of sensors.

4.1. Probability of missing the link flow inference of unobserved links

4.1.1. Identical sensors

The probability of missing the link flow observability of any observed link is equal to the probability of failure of the sensor installed on that link. However, for an unobserved link, the failure of at least one of the sensors installed in the

[3] For the proof, please refer to Castillo et al. (2014) or Xu et al. (2016).

observed links required for the link flow inference of that unobserved link can prevent the link flow inference of that link. According to Eq. (5), the flow of unobserved links can be inferred by multiplying the matrix $-T_u{}^{-1}T_o$ by the matrix of observed links, i.e., l_o. The elements of the matrix $-T_u{}^{-1}T_o$ can help us to identify the observed links that should be used for inferring the flow of an unobserved link. For instance, we can consider that the observed link j'' should be used to infer the flow of the unobserved link j' if the element $a_{j'j''}$ of row j' and column j'' of the matrix $-T_u{}^{-1}T_o$ is a non-zero value. The maximum probability of missing the link flow inference of an unobserved link can be obtained using Eq. (8):

$$Y_1 = \max_{j' \in J} \left(1 - \prod_{j'' \in J} \left(1 - a^2_{j'j''} p \right) \right) \tag{8}$$

where p represents the failure probability of identical sensors. Moreover, we squared the element of the matrix $-T_u{}^{-1}T_o$ in Eq. (8) to cancel the effect of negative signs for counting the number of observed links in each row of the matrix $-T_u{}^{-1}T_o$. Eq. (8) is helpful in identifying the unobserved links that have a higher chance of missing their link flow inference. When all sensors are identical, the probability of missing the link flow inference of an unobserved link depends on the number of observed links which need to be used to infer the flow of that unobserved link. In other words, the higher the number of observed links required for the link flow inference of an unobserved link, the higher the probability of missing the link flow inference of that link. We can identify the unobserved link(s) that need the maximum number of observed links for the link flow inference by counting the number of non-zero elements in each row of matrix $-T_u{}^{-1}T_o$.

In addition to determining the maximum possibility of missing the link flow inference of an unobserved link, we can also calculate the expected number of unobserved links whose flow cannot be inferred due to the failure of sensors installed on the observed links.

$$Y_2 = \sum_{j' \in J} \left(1 - \prod_{j'' \in J} \left(1 - a^2_{j'j''} p \right) \right) \tag{9}$$

By minimizing Y_2, we can reduce the expected number of unobserved links for which link flow cannot be inferred as a result of sensor failure. To obtain the average number[4] of observed links required for the link flow inference of each unobserved link, we can use the following equation:

$$Y_3 = \frac{\sum_{j'', j' \in J} a^2_{j'j''}}{|j'|} \tag{10}$$

where $|j'|$ is the number of unobserved links in a network. If a particular layout of sensors leads to a lower value of Y_3 compared to other layouts, then we expect this layout also has a lower value of Y_2 which means that this layout also has a lower expected number of unobserved links for which flow cannot be inferred due to the failure of sensors. The reason for this is the fact that Y_3 calculates the average number of observed links required to infer the flow of an unobserved link, and when sensors are assumed to be identical, the probability of missing the link flow inference of an unobserved link depends on the number of observed links needed to infer the flow of that link. Therefore, a lower value of Y_3 indicates that, on average, a smaller number of observed links are required for the link flow inference of unobserved links, and correspondingly, the lower the probability of missing the link flow inference of an unobserved link. However, if two layouts have the same value of Y_3, they could still have a dissimilar value of Y_2. We provide an example in Appendix I to discuss this situation in more details.

4.1.2. Non-identical sensors

Contrary to identical sensors, non-identical sensors can have different probabilities of failure depending mainly on their employed technology. The maximum probability of missing the link flow inference of an unobserved link in the presence of non-identical sensors can be calculated as follows:

$$Y_1'' = \max_{j' \in J} \left(1 - \prod_{f \in F} \prod_{j'' \in J} \left(1 - a^2_{j'j''} y_{fj''} p_f \right) \right) \tag{11}$$

where $y_{fj''}$ is a binary variable to determine if the sensor type f is installed on the observed link j'' or not, and p_f represents the failure probability of the sensor type f. Eq. (11) is of importance in detecting the unobserved link that has the highest chance of missing the link flow inference. In addition to the calculation of the maximum probability of missing the link flow inference, we can calculate the expected number of unobserved links whose flow will be missed due to the failure of non-identical sensors:

$$Y_2'' = \sum_{j' \in J} \left(1 - \prod_{f \in F} \prod_{j'' \in J} \left(1 - a^2_{j'j''} y_{fj''} p_f \right) \right) \tag{12}$$

[4] In this work, the term "average number" refers to the arithmetic mean of a variable.

where in Eq. (12), the higher value of Y''_2 indicates that the flow of a higher number of unobserved links cannot be inferred if one or more sensors installed on observed links break down.

4.2. Effect of a sensor failure on the link flow inference of unobserved links

4.2.1. Identical sensors

To discuss the effect of a sensor's failure on the link flow inference of unobserved links, we need to identify the appearance of observed links in different equations used to infer the flow of unobserved links. To determine the number of appearances of an observed link in these equations, we need to count the non-zero values of the column vector associated with that observed link in the matrix $-T_u{}^{-1}T_o$. Eq. (13) calculates the maximum expected number of unobserved links for which their flow will be missed due to the failure of a sensor installed on an observed link:

$$Y_4 = \max_{j'' \in J} \left(\left(\sum_{j' \in J} \alpha^2_{j'j''} \right) p \right) \tag{13}$$

In Eq. (13), $(\sum_{j' \in J} \alpha^2_{j'j''})$ counts the number of non-zero elements in the column vector associated with the observed link $j''$and it can show the number of appearances of the observed link j'' in different equations used for the link flow inference of unobserved links. We also can count the number of non-zero elements in each column vector of the matrix $-T_u{}^{-1}T_o$ to obtain the maximum number of observed links that is used in different equations required for the link flow inference. This way we can determine the maximum number of unobserved links for which their flow cannot be inferred due to the failure of a sensor installed on an observed link. The average number of unobserved links whose flow cannot be inferred due to the failure of a sensor can be calculated as:

$$Y_5 = \frac{\left(\sum_{j', j'' \in J} \alpha^2_{j'j''} \right)}{|j''|} \tag{14}$$

where in Eq. (14), $|j''|$ is the number of observed links in a network. Comparing Eqs. (14) and (10), we can conclude that by minimizing the average number of observed links used to infer the flow of an unobserved link, we can also minimize the average number of unobserved links where link flow cannot be inferred due to the failure of a sensor.

4.2.2. Non-identical sensors

For non-identical sensors, the expected number of unobserved links for which their flow cannot be inferred due to the failure of a sensor depends not only on the number of appearances of an observed link in different equations used for the link flow inference of unobserved links but also on the failure probability of the sensor installed on that observed link. The maximum expected number of unobserved links where their flow cannot be inferred due to the failure of a sensor is calculated as:

$$Y''_4 = \max_{j'' \in J} \left(\sum_{f \in F} y_{fj''} p_f \left(\sum_{j' \in J} \alpha^2_{j'j''} \right) \right) \tag{15}$$

where in Eq. (15), the observed link with the highest impact on the link flow inference of unobserved links can be identified.

5. Mathematical formulation

In this section, we present the constraints and objective functions required to determine the type and the location of sensors on links in a traffic network. To deal with the objective functions introduced in the previous section, we suggest using min-max and min-sum methods. Our mathematical formulation is introduced as follows:

Subscript

i	non-centroid node of a traffic network
j	links of a traffic network
j'	unobserved links of a traffic network
r	routes of a traffic network
j''	observed links of a traffic network
f	type of the sensor to be located on a link

Sets

I	set of non-centroid nodes: {1, .., $\|I\|$}
J	set of links in a traffic network: {1, .., $\|J\|$}
R	set of routes in a traffic network: {1, .., $\|R\|$}
M	set of major roads, $M \subset J$

F set of the sensor type to be located on links: {1, .., $|F|$}
H_i set of new links assigned to node i
H set includes all sets of new links {1, .., $|H|$}[5]

Parameters
T node-link incidence matrix ($T_{|I| \times |J|}$)
p_f probability of failure of sensor type f
c_f cost of sensor type f that can be located on a link
w_j relative importance of link j
h_{ij} a binary parameter that shows if link j is assigned to the set of new links associated with the node i, i.e., $h_{ij}=1$ if $j \in H_i$
q_{jr} a binary parameter that shows if route r traverses link j or not. $q_{jr}=1$ if route r traverses link j and $q_{jr}=0$ otherwise
ϑ Budget constraint

Decision variables
x_{ij} binary variable indicating whether link j which is assigned to the node i as a new link is an unobserved link ($x_{ij}=1$) or not ($x_{ij}=0$).
o_j binary variable determining if link j is an observed link or not.
y_{fj} binary variable indicating whether the sensor type f is installed on link j ($y_{fj}=1$) and ($y_{fj}=0$) otherwise.
T_u variable associated with a set of column vectors structured by selecting a link from each set of new links and putting the column vector related to that link from node-link incidence matrix in T_u. The binary variable o_j associated with each link selected to be in T_u should be equal to zero.

5.1. Objective functions and constraints regarding identical roads

To install sensors in a network, we can assume all links are equally significant and find the preferred location of sensors so as to minimize the effect of sensor failure on the link flow inference. The reason for introducing the min-max functions is to minimize the maximum effect of sensor failure on the link flow inference of unobserved links. Depending on whether sensors are identical or not, we can define different min-max objective functions to identify the location of sensors. Eq. (16) introduces two possible objective functions assuming that sensors are not identical.

$$\begin{cases} Z_1 = \min\left(\max_{j' \in J}\left(1 - \prod_{f \in F}\prod_{j'' \in J}\left(1 - a^2_{j'j''} y_{fj''} p_f\right)\right)\right) & \text{I} \\ Z_2 = \min\left(\max_{j'' \in J}\left(\sum_{f \in F} y_{fj''} p_f \left(\sum_{j' \in J} \alpha^2_{j'j''}\right)\right)\right) & \text{II} \end{cases} \tag{16}$$

Eq. (16)-I) minimizes the maximum probability of not inferring the flow of an unobserved link due to the failure of sensors, while Eq. (16)-II) minimizes the maximum effect of a sensor's failure on the link flow inference of unobserved links. Eq. (16) can be used for identical sensors by considering that $p_f = p, \forall f$ and excluding the binary variable from the equation that determines the type of sensor installed on an observed link. The min-sum objective function is introduced here to minimize the average number of unobserved links whose link flow inference will be affected by a sensor's failure. To be more specific, we introduced Eq. (17) to minimize the expected number of unobserved links whose flow cannot be inferred due to the failure of sensors.

$$Z_3 = \min\left(\sum_{j' \in J}\left(1 - \prod_{f \in F}\prod_{j'' \in J}(1 - a^2_{j'j''} y_{fj''} p_f)\right)\right) \tag{17}$$

similar to Eq. (16), Eq. (17) can be used for identical sensors, assuming all sensors have the same probability of failure and by removing the binary variable y_{fj} from the equation. The following constraints relate to the above mentioned objective functions:

s.t.,

$$\sum_{j \in H_i} h_{ij} x_{ij} = 1 \qquad \forall i \in I \tag{18}$$

$$1 - \sum_{i \in I} x_{ij} = o_j \qquad \forall j \in J \tag{19}$$

$$\sum_{f \in F} y_{fj} = o_j \qquad \forall j \in J \tag{20}$$

[5] Based on the definition of the set of new links, the inequality $|H| \leq |I|$is always valid.

$$\sum_{j\in J}\sum_{f\in f} c_f y_{fj} \le \vartheta \tag{21}$$

constraint (18) allows a link to be an unobserved link in the set of links assigned to the node i, if that link is already available in the set of new links associated with node i. Constraint (19) identifies the set of observed links in a network that should be equipped with sensors. According to constraint (20), if a link is considered as an observed link in any set of new links, then the flow of that link should be observed by a sensor installed on that link. Constraint (21) imposes the budget constraint required for installing sensors in a network, while the budget should be sufficient to allow installation of the minimum number of sensors required for full link flow observability.

5.2. Objective functions and constraints considering major roads

In real networks, all links are not of the same importance –some are major roads, such as highways or major arterials, and others are minor roads such as collectors. Regarding the failure of sensors, we are interested in incorporating the relative importance of links in finding the optimal location of sensors. On one hand, if the number of links required to be instrumented with sensors exceeds the number of major links in a network, then traffic sensors can be manually assigned to all major roads, i.e., major roads become observed links, and the rest of the observed links can be selected from the remaining links in the set of links. This assignment can be justified by the fact that the chance of missing the link flow inference of an unobserved link is usually higher than the chance of missing the link flow observability of an observed link. The rest of the links required to complete the set of observed links can be selected from the minor roads in a network while using the min-max or min-sum objective functions introduced in Eqs. (16) and (17), respectively. On the other hand, if the number of links required to be equipped with sensors is less than the number of links in the set of major roads, then either of Eq. (16) or (17) can still be used as the objective function of the model while enforcing that all members in the set of observed links should be from the set of major roads. The following are the objective function and constraints that consider major roads in instrumenting links with sensors for the two situations described above:

$$Z_4 = \min\left(\sum_{j'\in J}\left(1-\prod_{f\in F}\prod_{j''\in J}\left(1-a^2_{j'j''}y_{fj''}p_f\right)\right)\right) \text{OR} \begin{cases} Z_1 = \min\left(\max\limits_{j'\in J}\left(1-\prod\limits_{f\in F}\prod\limits_{j''\in J}\left(1-a^2_{j'j''}y_{fj''}p_f\right)\right)\right) & \text{I} \\ Z_2 = \min\left(\max\limits_{j''\in J}\left(\sum\limits_{f\in F} y_{fj''}p_f\left(\sum\limits_{j'\in J}\alpha^2_{j'j''}\right)\right)\right) & \text{II} \end{cases} \tag{22}$$

s.t.

Eq. (20) & Eq. (21)

$$\begin{cases} \sum\limits_{f\in F} y_{fj} = 1 \quad \forall j\in M \quad \text{if } |M| \le |J| - |H| & \text{I} \\ \text{OR} \\ \sum\limits_{f\in F} y_{fj} = 0 \quad \forall j\in J\setminus M \quad \text{if } |M| > |J| - |H| & \text{II} \end{cases} \tag{23}$$

$$\sum_{j\in J} o_j = |J| - |H| \qquad \text{if } |T_u| \neq 0 \tag{24}$$

as we explained above, the objective function selected to be used in both situations can be either Eq. (16) or Eq. (17). Constraint 23-I) is associated with the case where the number of major links is less than the number of observed links required to reach full link flow observability, while, constraint (23-II) is formulated for the case where the number of major roads is greater than the number of observed links required to guarantee full link flow observability. Constraint (24) ensures that the number of observed links is equal to the number of links minus the total number of sets of new links. According to this constraint, the observed links should be selected in a way that the node-link incidence matrix related to unobserved links has a non-zero determinant. This non-zero determinant condition needs to be satisfied, because by enforcing that the set of observed links be from the set of major roads, it is possible that more than one link in a set of new links is selected as the unobserved link which means the concept of new links explained in Section 3.1 cannot be applied.

Moreover, equipping all major roads with sensors could also lead to a situation where it is not possible to construct the matrix of unobserved links to be invertible. We provide an example in the small Fishbone network in Appendix II to elaborate on this situation in more detail. To avoid the occurrence of the above-mentioned situation, we could update the sets of new links by removing the major links to be instrumented with sensors from the sets of new links in such a way as to avoid a set of new links becoming an empty set. Employing this approach, we can still use the concept of new links to generate initial feasible solutions. However, as Eq. (23) is no longer applicable to this approach, we need to relax this constraint as well as update the objective function to cause more major links to become observed links in the optimum

solution. A possible way to achieve this objective is to assign weights to links to signify their relative importance considering different factors including the capacity of links and so on. The updated objective function is provided below:

$$Z_5 = \min\left(\sum_{j'\in J} w_{j'}\left(1-\prod_{f\in F}\prod_{j''\in J}\left(1-\left(a^2_{j'j''}y_{fj''}p_f\right)\right)^{\frac{1}{w_{j''}}}\right)\right) \tag{25}$$

where in Eq. (25), $w_{j''}$ and $w_{j'}$, $(0 < w_{j''}, w_{j'} \le 1, \forall j'', j' \in J)$ are the weights assigned to a link in a traffic network to emphasize the relative importance of the link, with higher values of the weight for a link indicating greater significance of that link. In Eq. (25), if a link is unobserved, then its relative weight is equal to $w_{j'}$. In this way, the objective function assigns the links with lower weights as unobserved links to minimize the value of Z_3. Moreover, if the link becomes an observed link, then its weight is represented as $\frac{1}{w_{j''}}$ as the power of the term $(1-(a^2_{j'j''}y_{fj''}p_f))$, $0 \le (1-(a^2_{j'j''}y_{fj''}p_f)) \le 1 \forall j'', j' \in J, f \in F$, to maximize this term and to prompt the model to assign the links with higher weights as observed links. Considering Eq. (25) as the objective function, then we should set Eqs. (18-21) as the constraints of the model. Eq. (25) is also useful for the situation where it is easier to incorporate the relative importance of links compared to each other, instead of separating the links into two distinctive sets of major roads and minor roads. Employing Eq. (25) as the objective function and Eqs. (18-21) as the constraints, we also can directly construct the set of unobserved links from the original sets of new links, not the updated ones.

6. Full link flow observability considering route flow information

Although access to route flow information in the strategic planning phase of a network is not always feasible, this type of information can provide urban planners with useful knowledge to reduce the number of sensors required to be installed in a network (Fu et al., 2016). Note that our aim in this section is not to separately investigate the full/partial route flow observability problem considering the failure of sensors, but to discuss how the existence of route flow information will lead to a better evaluation of the solutions to reach full link flow observability, which is the main focus of this work. Depending on the uniqueness of information that can be obtained from link flow observation, routes can be divided into three distinctive sets:

R^1: All links traversed by this type of route are not traversed by any other route.
R^2: There is at least one link in the set of links traversed by route type 2 which is not traversed by any other route.
R^3: All links traversed by route type 3 are also traversed by other routes.

Note that the definition of route types, i.e., sets R^1, R^2 and R^3, is analogous to that provided by Rinaldi and Viti (2017). They also categorized routes into three categories; namely, non-redundant routes (NR), redundant while informative routes (RI), and purely redundant (PR) routes. The definition of categories NR, RI and PR routes are very similar to sets R^1, R^2 and R^3, respectively. One important difference is that Rinaldi and Viti (2017) defined a route as belonging to NR category if the links traversed by it were not *previously* crossed by any other route, whereas in our definition, a route is classified as type 1 if the links traversed by that route are not crossed by *any other* route. We proposed this definition for R^1 as it makes it easier to interpret the failure effect of sensors installed on links. Eq. (26) represents the characteristics of sets R^1, R^2 and R^3:

$$\begin{cases} R^1 \cap R^2 = \varnothing & \text{I} \\ R^1 \cap R^3 = \varnothing & \text{II} \\ R^2 \cap R^3 = \varnothing & \text{III} \\ R^1 \cup R^2 \cup R^3 = R & \text{IV} \end{cases} \tag{26}$$

According to Eq. (26), there is no intersection between any pair of sets R^1, R^2 and R^3. Moreover, Eq. (26-IV) declares that the union of sets R^1, R^2 and R^3 equals R which is the set of all routes in a network.

The flow of a link in a network can consist of the summation of flow of routes from sets R^1, R^2 or R^3. The following equation demonstrates the relationship between flow of routes which traverse link j:

$$v_j = \sum_{r\in R^1\cup R^2\cup R^3} e_r \tag{27}$$

where e_r is the ongoing flow of route r. In Eq. (27), if r, where $r \in R^1 \cup R^2$, is the only route traversing link j, then by instrumenting link j with a sensor, we can obtain the flow of this route. In a different situation, if $r \in R^2 \cup R^3$ and there is more than one route crossing link j, then we may still find the exact flow of all or some routes traversing link j by equipping this link with a sensor while also using the route information obtained from other routes in R^1 and R^2. This latter situation is discussed by Castillo et al. (2014) and Rinaldi and Viti (2017) when they addressed the fact that a route in the set of R^3 may still contribute to increasing the gain in route information by using sensor-equipped link information. In other words, these authors pointed out that considering link-route incidence matrix, the column vector related to the route r' in R^3 may be independent from the union of column vector of routes in $R^1 \cup R^2$. Rinaldi and Viti (2017) identify those routes

in R^3 in a network to ensure there is no other route that can contribute to partial/full route flow observability. In our work, we suggest installing a sensor on at least one link from the set of links traversed by each route in R^1:

$$\sum_{j\in J} q_{jr} o_j \geq 1 \qquad \forall r \in R^1 \tag{28}$$

In Eq. (28), q_{jr} is a binary parameter that shows whether route r traverses link j or not. The value of this parameter can be obtained from the link-route incidence matrix. Moreover, for the set of links traversed by a route in R^2, we recommend equipping the link which is not traversed by other routes with a sensor:

$$q_{jr} - \left(\sum_{r'\in R\setminus\{r\}} q_{jr'} \right) \leq o_j \qquad \forall j \in J, r \in R^2 \tag{29}$$

according to Eq. (29), if a link is traversed by a route in R^2, and is not traversed by any other route in R, then that link should be equipped with a sensor. Finally, by using the results of the model developed by Rinaldi and Viti (2017), we can recognize which routes in R^3 are contributing to route flow observability and install a sensor on at least one of the links traversed by these routes:

$$\sum_{j\in J} q_{jr} o_j \geq 1 \qquad \forall r \in R^{3'} \tag{30}$$

where $R^{3'}$ is the set of routes in R^3 which are independent from all routes in R^1 and R^2. According to Eq. (30), at least one of the links available in the set of links traversed by a route in $R^{3'}$ should be instrumented with a sensor.

We should note that we may not be able to reach full link flow observability employing Eqs. (28)–(30) as hard constraints. This situation could arise when the set of links which create a cyclic graph are selected to be instrumented with sensors according to these three constraints.[6] To avoid this possibility, we suggest finding the location of sensors to reach full link flow observability in the first level optimization and then maximizing the information gain of routes, i.e., minimizing the probability of missing the route flow observability in the second level by using the pool of optimum solutions obtained in the first level as feasible solutions for the second level optimization. We also can combine both objective functions, including minimizing the effect of sensor failure on link flow inference of unobserved links, as well as minimizing the effect of this failure on route flow observability of routes in a single level optimization, using weighted sums method (WSM) or ε-constraint. However, we prefer two-level optimization as the feasible solution used in the second level guarantee to position sensors in a way to have minimum failure effect on link flow inference of unobserved links. The objective function and the constraint of the second level can be defined as:

$$Z_6 = \sum_{r\in R^1\cup R^2\cup R^{3'}} \left(\prod_{j\in J} \prod_{f\in F} (p_f)^{y_{fj} q_{jr}} \right) \tag{31}$$

s.t.

Eqs. (18-21)

$$\begin{cases} Z_4 \leq Z_4^{opt} & \text{I} \\ OR & \\ Z_5 \leq Z_5^{opt} & \text{II} \end{cases} \tag{32}$$

Eq. (31) attempts to minimize the expected number of routes in R^1, R^2, and $R^{3'}$ for which route flow observability will be missed due to the failure of sensors. According to this equation, the flow of a route will be missed if all sensors installed on links traversed by this route break down. In other words, the higher the number of sensor-equipped links traversed by a route, the lower the probability of missing that route flow observability. In the second level optimization, Eqs. (18-21) are employed to ensure full link flow observability. Moreover, Eq. (32) ensures that, depending on the objective function used in the first level optimization, i.e., Z_4 or Z_5, the optimum solution of the second level is also the optimum solution of the first-level optimization model.

7. Redundant sensors in a traffic network

After identifying the location of sensors, we can also investigate the preferred location of *redundant sensors* – the *minimum* number of extra sensors needed to maintain the full link flow observability of a network if one or more of the sensors installed on observed links fails to observe the link flows. These redundant sensors provide us with two main benefits for traffic monitoring purposes: (1) most importantly, they can maintain full link flow observability when sensor failure occurs

[6] Please refer to Appendix II where we discuss a similar situation in which instrumenting all major links with sensors leads to the creation of a cyclic graph.

in the system; thus, adding to the robustness of the network observability and (2) to a lesser degree, they can participate in reducing the link flow inference error when there is no failure among sensors in a network. We developed the idea of redundant sensors in this work to account for the possibility of sensor failure when the initial location of sensors is determined using the optimization model introduced in Section 5. The following steps outline the procedure required for finding the type and location of redundant sensors:

Step 1. Determine the initial location of sensors

According to this step, we need to determine the optimum location of sensors to reach full link flow observability. The objective function and the constraint introduced in Section 5 can be employed to find the location of sensors.

Step 2. Consider all combinations of failure among sensors

This step mainly deals with the possible failure of sensors already installed on links according to Step 1. For instance, if we assume layout A introduced in the motivating example as the optimum location of sensors determined in Step 1, then in Step 2, we need to find each possible combination of failure between these installed sensors. According to layout A, in which there are 12 sensors installed in the Fishbone network, we need to consider $2^{12}-1$ combinations of failure among sensors. However, considering all failure combinations presents its own combinatorial complexity and might not be feasible for relatively large networks. To deal with this situation, we suggest considering the failure combinations among sensors that are most susceptible to failure. Moreover, as already discussed, we suggest examining the failure of only those sensors installed on major roads as these roads are more important for traffic monitoring purposes.

Step 3. Find the location of redundant sensors for each combination of failures

Step 3 attempts to find the location of redundant sensors for each combination of sensor failure determined in Step 2. To find the location of these extra sensors, we use the objective functions and the constraints introduced in Section 5. However, we need to add the following constraints as well:

i The redundant sensors cannot be installed on a link which already has failed sensors.
ii The location of sensors, excluding the redundant sensors, should follow what we already determined in Step 1.

For instance, considering layout A introduced in the motivating example, we know that one of the possible combinations of failure is the situation in which sensors installed on links 3 and 5 stop functioning. Considering this scenario, according to Step 3, we need to find the location of extra sensors in the Fishbone network to reach full link flow observability using the optimization model introduced in Section 5. The new constraints that should be considered include the fact that redundant sensors cannot be installed on links 3 and 5 anymore (constraint *i*) and that the rest of the sensors, excluding the redundant sensors, should follow the sensor positioning introduced in layout A (constraint *ii*). Note that depending on the network topology, we can disregard some of the combination of failures among sensors determined in Step 2 as the link flow observability is impossible in those situations.

Step 4. Sensor assignment

In this step, we use the results obtained from Step 3 which specify the location of redundant sensors for each combination of sensor failure. In Step 4, we assigned sensors to links based on the frequency of being selected in Step 3. This means that the links that have been selected more often to be instrumented with redundant sensors will be equipped with more advanced sensors. The sensor assignment, however, is subject to budget constraints which limit the type of sensors to be installed on links as well as the number of links to be equipped with sensors.

8. Solution algorithm

The optimization problem presented in Section 5 is a nonlinear problem. The nonlinearity arises in the objective functions introduced in Eqs. (16) and (17) [presented altogether in Eq. (22)], Eq. (25) and (31). Moreover, due to the existence of binary decision variables y_{fj} and o_j, it becomes an integer optimization problem. The combinatorial complexity introduced in the problem is due to the fact that there is no general and explicit function to express the relationship between the sensor location scheme and the number of observed links required for link flow inference of unobserved links. Moreover, with respect to redundant sensors, there is a scalability concern introduced in Step 2 that motivates us to employ an efficient solution algorithm to solve the proposed problem.

To solve the proposed optimization problem, we employed the progressive genetic algorithm (GA) initially developed by Guan and Aral (1999) which is designed for optimization problems with nonlinear equality and inequality constraints. The output of the GA is the location of observed links in a traffic network to reach full link flow observability, as well as the type of sensors to be installed at these locations in the case of non-identical sensors. Note that we implemented the proposed GA using MATLAB R2014 software on a personal computer with 3.4 GHz Intel Core^{TM} i7-6700 processor and 16GB of memory.

Fig. 3 provides the flow chart of the employed algorithm. According to the figure, the algorithm initiates with the initialization procedures, in which the required inputs, chromosome representation approach, and population sizes are defined. Note that all parameters introduced in Section 5 will be the input of the GA in the initialization procedure. Moreover, in the initialization procedure, we built three different initial populations introduced as P^1, P^2&P^3 with distinctive sizes depending on the size of a network to find the best number of iterations and also to assure we reached the best possible solution. This step is followed by chromosome evaluation, i.e., sorting, using fitness functions. The fitness function introduced as $Z_{Fitness}$ is used in a GA to guide the simulation procedure toward optimal solutions. Crossover and mutation procedures are then employed to reproduce more premium chromosomes and to keep the diversity of feasible solutions, respectively. In the next

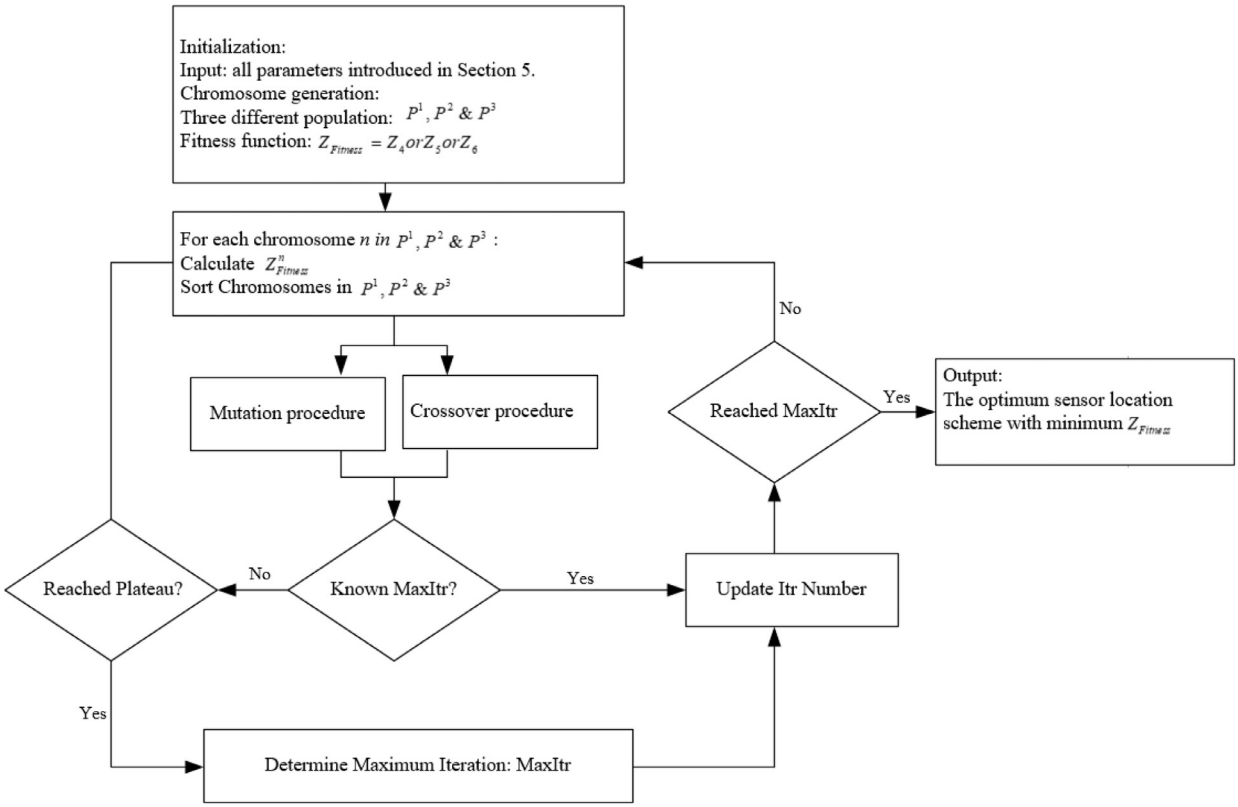

Fig. 3. Flowchart of the algorithm.

Table 4
Settings related to the proposed GA.

Parameters	Description
Initial population size	Three different population sizes. Population size varies depending on the size of network
Mutation rate	Discrete uniform distribution. Range: [0.2, 0.7]
Crossover rate	Discrete uniform distribution. Range: [0.4,0.9]
Number of iteration (*MaxItr*)	4 × the maximum repetition among different populations

steps, the number of iterations introduced as "MaxItr" is determined by evaluating the points for each initial population in which the fitness function reaches a plateau.

Table 4, below describes the parameter settings related to the proposed GA. The lower and upper bounds of the possible range of crossover rate are higher than for mutation rate as we will give the chromosomes with higher fitness value a higher chance of reproduction. Note that we provide explanations related to the number of iterations in Section 8.4.

In the following section, we provide in-depth details related to GA structure, as well as the approach used to deal with nonlinearity of objective functions.

8.1. Chromosome generation and representation

In the designed GA, a chromosome length equals the number of links in a network. The cells associated with the randomly selected links from each set of new links, which are considered as the unobserved links, should be set to zero. For the remaining cells of the chromosome, a type of sensor is randomly selected and the number given in each cell represents the sensor type that should be installed on that link. For instance, if the j^{th} cell of a chromosome is equal to f, it means that the sensor type f should be installed on link j. For the initial population, we used the concept of new links to avoid an exhaustive search in generating feasible solutions, while allowing more than one link to be selected from each set of new links in subsequent populations to keep the diversity of possible solutions. The feasibility of solutions is then evaluated considering the budget constraint introduced in Eq. (21) as well as determining if the matrix of unobserved links, i.e., T_u, is an invertible matrix.

8.2. Fitness function

In the proposed GA, Eqs. (16), (17), (25) or (31) can be used as the fitness function. However, the nonlinearity in these objective functions can contribute to the runtime of the proposed algorithm. So, we attempted to linearize these functions in order to decrease the running time as much as possible. This process of linearization is explained for Eq. (17), while a similar approach can be chosen to linearize other objective functions. One of the variables that contributes to the nonlinearity of Eq. (17) is $a_{j'j''}$, which could be −1, 0 or 1. In Eq. (17), $a_{j'j''}$ is taken to the power of 2 which reduces the possible values for this variable to be either 0 or 1. We introduced a new binary variable, $\beta_{j'j''}$, that takes the value of 1 if $|a_{j'j''}| = 1$ and 0 otherwise. Eq. (17) can be rewritten using this new binary variable:

$$Z_3 = \min\left(\sum_{j'\in J}\left(1-\prod_{f\in F}\prod_{j''\in J}\left(1-\beta_{j'j''}y_{fj''}p_f\right)\right)\right) \tag{33}$$

where in Eq. (33), the term $\prod_{f\in F}\prod_{j''\in J}(1-\beta_{j'j''}y_{fj''}p_f)$ includes the multiplication of two binary variables, i.e., $\beta_{j'j''}$ and $y_{fj''}$, that can be replaced with a new binary variable $\eta_{j'j''f}$. By including the variable $\eta_{j'j''f}$, we also need to consider the following constraints:

$$\eta_{j'j''f} \le \beta_{j'j''} \qquad \forall j', j'' \in J, f \in F \tag{34}$$

$$\eta_{j'j''f} \le y_{fj''} \qquad \forall j', j'' \in J, f \in F \tag{35}$$

$$y_{fj''} + \beta_{j'j''} - 1 \le \eta_{j'j''f} \qquad \forall j', j'' \in J, f \in F \tag{36}$$

Eqs. (34) and (35) restrict the value of$\eta_{j'j''f}$ to be zero when either of$y_{fj''}$ or $\beta_{j'j''}$ is zero. Moreover, according to Eq. (36), $\eta_{j'j''f}$ is equal to 1 when both $y_{fj''}$ and $\beta_{j'j''}$ are 1. The new illustration of Eq. (33) will be as follows:

$$Z_3 = \min\left(\sum_{j'\in J}\left(1-\prod_{f\in F}\prod_{j''\in J}\left(1-\eta_{j'j''f}p_f\right)\right)\right) \tag{37}$$

The next step is to linearize the multiplications terms in $\prod_{f\in F}\prod_{j''\in J}(1-\eta_{j'j''f}p_f)$. We employed the log function to linearize this term and replaced the linearized form in Eq. (37):

$$Log\left(\prod_{f\in F}\prod_{j''\in J}(1-\eta_{j'j''f}p_f)\right) = \sum_{f\in F}\sum_{j''\in J}\mathrm{Log}\left(1-\eta_{j'j''f}p_f\right)\forall j'\in J \Rightarrow Z_3' = \min\left(\sum_{j'\in J}\left(1-\sum_{f\in F}\sum_{j''\in J}\mathrm{Log}\left(1-\eta_{j'j''f}p_f\right)\right)\right) \tag{38}$$

Eq. (38) represents the linear form of Eq. (17) which means that the minimum value of Z_3' also guarantees the minimum value of Z_3. Note that we employed the linear form of objective functions to solve the illustrative examples.

8.3. Mutation and crossover procedures

The single-point crossover procedure is applied to the proposed GA to increase the chance of reproduction of the chromosomes that stand in a higher rank considering the fitness function. Moreover, the mutation procedure is employed to keep the genetic diversity in the generation of a population. In both the mutation and crossover procedures, the chromosomes are allowed to select links as unobserved links which do not necessarily originate from the set of new links.

8.4. Stopping criteria

The generational process in GA is repeated until a termination condition is reached. The common terminating conditions are satisfying predefined criteria, reaching a fixed number of repetitions, reaching the budget cap, and reaching no improvement in the fitness function through successive iterations. In this work, among all the above mentioned conditions, we consider the number of repetitions to terminate the GA. Based on this condition, the GA stops when it reaches the number of repetitions determined as an input. Note that we repeated the GA with different initial populations and defined the number of repetitions as four times the maximum repetition among different populations in which the highest-ranking solution reaches a plateau such that successive iterations no longer produce better results. This approach is a useful method to avoid exhaustive iterations when there is a low probability of reaching a better solution.

Table 5
Data related to the sensors used for the illustrative networks.

Sensor type	Parameter values		
	Probability of failure		Cost per sensor ($\times$100\$)[b]
	HVL < 3.5% TL[a]	HVL > 3.5% TL	
1 (Basic)	0.5	0.8	120
2 (Advanced)	0.3	0.6	180

[a] TL stands for total traffic load in the urban area.
[b] From Table 5 on, cost mentioned in this work should be multiplied by 100.

9. Illustrative examples

This section includes three illustrative cases to examine the applicability of the proposed model for various networks with different topologies and sizes. The first example is the Fishbone network which is already introduced in the motivating example in Section 2. The second case, the Sioux Falls network, belongs to the city of Sioux Falls in the state of South Dakota, United States, and is a well-known network in transportation research which has been studied by many scholars (e.g. Ng, 2012; Xu et al., 2016). Finally, to further demonstrate the applicability of the proposed model, we studied the network of the city of Irvine, California in the United States. In this network, we cover the majority of roads in Irvine, especially the central section and west side of the city. This network has been used as a benchmark for solving many problems including the traffic counting location problem (Chootinan et al., 2005; Xu et al., 2016; Zhou and List, 2010), AVI location problem (Fei et al., 2007; Zhou and List, 2010) and OD estimation problem (Chen et al., 2009; Chootinan and Chen, 2011).

In this work, we assumed that two types of sensors can be installed in a network. Table 5 shows the probability of failure and cost of two types of sensor. The two sensor types have a different probability of failure depending on the employed technology and price range. The Traffic Detector Handbook identified different sources of failure for loop detectors which is one commonly used type of counting sensor (Klein et al., 2006). According to this handbook, wire breakage due to pavement failure is one of the primary reasons for loop detector failure.[7] This handbook, as well as the book entitled "Effects of heavy-vehicle characteristics on pavement response and performance" by Gillespie (1993), emphasized the effect of heavy vehicles on pavement failure. As our focus in this work is on the failure of counting sensors, which also include loop detectors, we took into consideration whether or not a link is often traversed by heavy vehicles. The Federal Highway Administration (FHWA) also defined 15 classes of vehicle among which classes 2 through 13 can be considered as heavy vehicle classes including buses and 2–7 axle trucks (Hallenbeck et al., 2014). The 2015 Urban Mobility Scorecard Report (2015) stated that heavy vehicles from classes 3 to 13 constitute up to 7% of traffic load in urban areas in Unites States. This percentage shows the maximum load of heavy vehicles which can contribute to pavement failure. In this work, for the sake of simplicity, we assumed that if the percentage of heavy vehicles passes a certain threshold of traffic load (i.e., 3.5%), then the probability of sensor failure on that roadway increases correspondingly. This threshold was selected following the logic that if the HVL exceeds 50% of the maximum loads of heavy vehicles (i.e., 7%), then sensor failure increases accordingly.

9.1. Full link flow observability: Fishbone network

The minimum number of sensors required to be installed on the links of the Fishbone network is 12 to reach full link flow observability as already discussed in the motivating example. If all 12 sensors are selected from sensor type 1, which has a lower cost compared to sensor type 2, then the total budget required for installing these 12 sensors is 1440\$. This means that the budget cannot be less than 1440\$ in order to reach full link flow observability. However, if the budget cap is more than 1440\$ then some of the sensors to be installed on observed links can be selected from the sensor type 2 category which has a higher cost but offers a lower probability of failure.

Fig. 4 illustrates the results related to the min-max objective function introduced in Eq. (16-I) that attempts to minimize the maximum probability of missing the link flow inference of unobserved links. As explained in Section 4.1.1, when the sensors are assumed to be identical, this objective function is equivalent to minimizing the maximum number of observed links required for the link flow inference of an unobserved link. The vertical axis represents the maximum number of observed links that need to be used for the link flow inference of an unobserved link in the Fishbone network. In this figure, we examine the proposed GA for three different populations having a dissimilar number of chromosomes in their initial pool of solutions. According to Fig. 4, the first population that has a smaller initial population size, i.e. lower number of chromosomes in the initial pool, takes a larger number of iterations, 88 iterations, to reach to the optimal solution obtained from the second and third populations with fewer iterations. According to the stopping criteria described in Section 8.4, we multiplied the maximum number of iterations among all three populations by four to reach a plateau to determine the number of iterations required to terminate the proposed GA. In this case, as this maximum value belongs to the first population, we multiplied 88 by 4 to obtain the number of sufficient iterations required for minimizing the maximum number of

[7] Based on a survey of more than 15,000 loop installations in the state of New York.

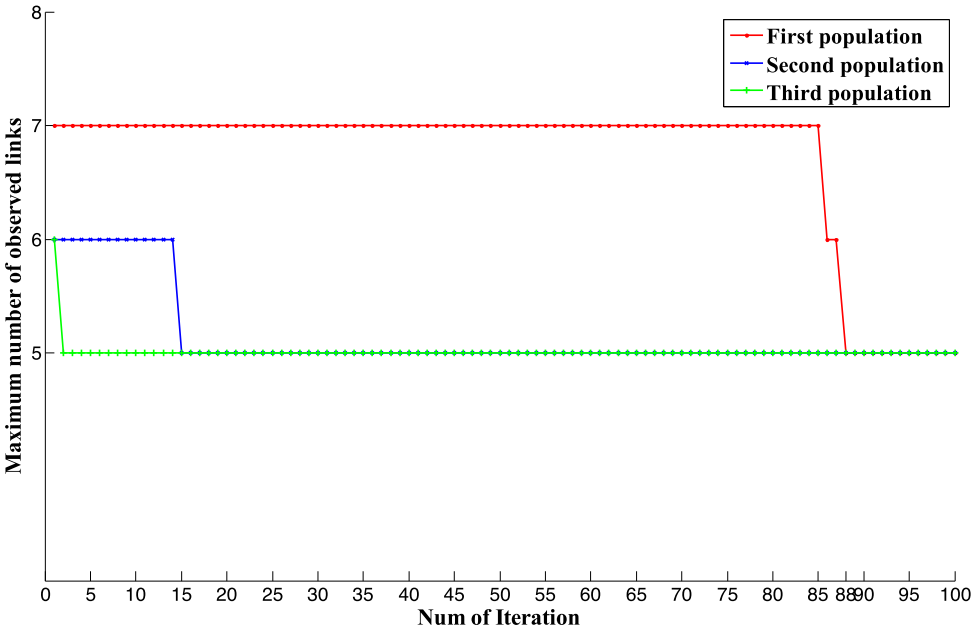

Fig. 4. The maximum number of observed links required for link inference of an unobserved link in the Fishbone network using different initial populations.

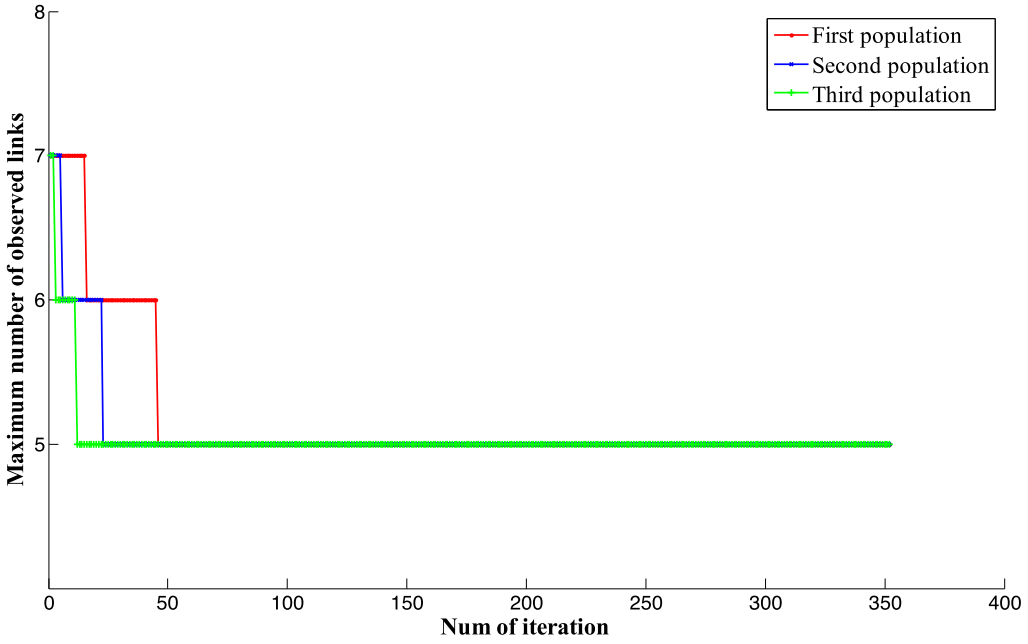

Fig. 5. The maximum number of observed links required for link inference of an unobserved link in the Fishbone network using the required number of iterations.

observed links used for the link flow inference of an unobserved link in the Fishbone network. Fig. 5 illustrates the results related to all three populations when the number of iterations is set to 352. We repeated the equivalent procedure introduced in Figs. 4 and 5 for determining the sufficient number of iterations while using different objective functions in the following tables and figures.

Table 6 shows the results of applying the min-max and min-sum objective functions for the Fishbone network assuming that all sensors are identical. The objective function defined for the first layout of this table is consistent with Eq. (16-I) and is defined to minimize the maximum number of observed links required for the link flow inference of an unobserved link. For the second layout, the objective function is defined based on Eq. (16-II) and aims at minimizing the maximum number

Table 6
Suggested layouts for the Fishbone network using identical sensors.

Layout No.	Objective function	Set of unobserved links	No. of observed links[a]		No. of unobserved links[b]	
			Avg	Max	Avg	Max
1	Z_1	{2, 7, 8, 11, 14, 17}	3.83	**5**	1.92	4
2	Z_2	{2, 7, 10, 12, 13, 16}	4.16	7	2.08	**3**
3	Z_3, s.t. $\begin{cases} Z_1 \le 5 \\ Z_2 \le 3 \end{cases}$	{3, 6, 7, 11, 12, 17}	3.67	5	**1.83**	3

[a] Number of observed links required for the link flow inference of an unobserved link.
[b] Number of unobserved links whose link flow inference depends on an observed link.

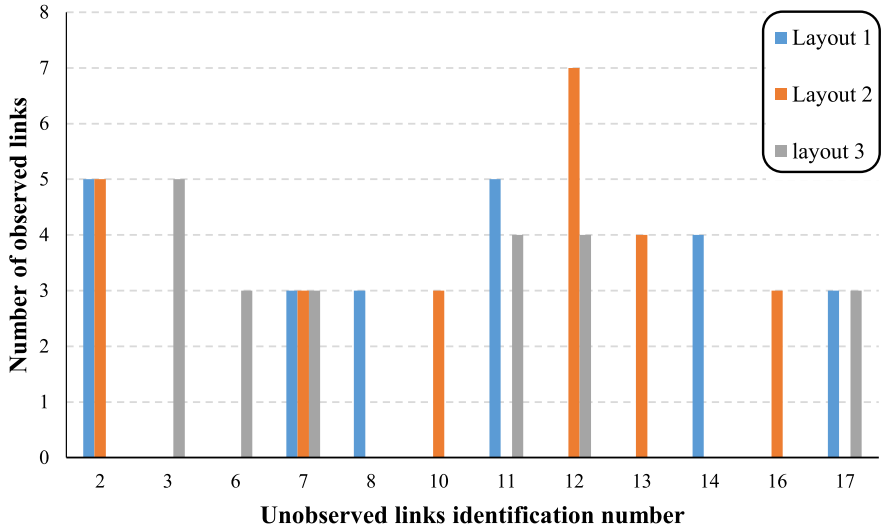

Fig. 6. The number of observed links required for link inference of each unobserved link.

of unobserved links whose flow cannot be inferred due to the failure of a sensor. For each objective function, the highlighted value in the corresponding row is the objective function value. For instance, the maximum number of unobserved links for which their flow cannot be inferred due to the failure of a sensor is three according to the highlighted result associated with the second layout. The third layout suggested for the Fishbone network in Table 6 is based on the objective function introduced in Eq. (17), and the results of Z_1 and Z_2 related to the first and the second layouts, respectively are set as the constraints. The results of the third layout demonstrate improvements in the average number of observed links for the link flow inference of each unobserved link as well as the average number of unobserved links whose link flow inference depends on an observed link when the constraints related to Z_1 and Z_2 are satisfied. Note that the results presented in Table 6 using the GA algorithm are achieved in 5 to 7 s.

Fig. 6 illustrates the number of observed links required for the link flow inference of each unobserved link in different sets of unobserved links for each layout introduced in Table 6. According to this figure, unobserved links 2 and 11 require the maximum number of observed links, i.e., five observed links, for their link flow inference in the first layout of Table 6. However, in the second layout of this table, the maximum number of observed links required for the link flow inference of the unobserved link 12 increases to seven. The main source of this difference in the maximum number of observed links for the link flow inference of an unobserved link in the first and in the second layouts relates to the objective functions defined for these layouts. In the first layout, the objective function is consistent with minimizing the maximum number of observed links in each equation used for the link flow inference of unobserved links, while in the second layout, the objective function tends to minimize the maximum number of unobserved links whose link flow inference depends on an observed link. For the third layout, the maximum number of observed links in an equation cannot exceed five observed links as it is defined as a constraint for this layout and according to Fig. 6, only unobserved link 3 requires five unobserved links for its link flow inference. For a particular layout, if there is no bar for a given link in the horizontal axis of Fig. 6, then it means that this link is not an unobserved link in that layout. For instance, there is no blue or orange bar for link 6 in Fig. 6, which means that link 6 is not an unobserved link in layouts 1 and 2.

Fig. 7 demonstrates a comparison between the first, second and third layouts in Table 6 concerning the appearance of observed links in different equations used for the link flow inference of unobserved links. The reason for this comparison is to study the effect of a sensor's failure on the link flow inference of unobserved links. According to this figure, the observed

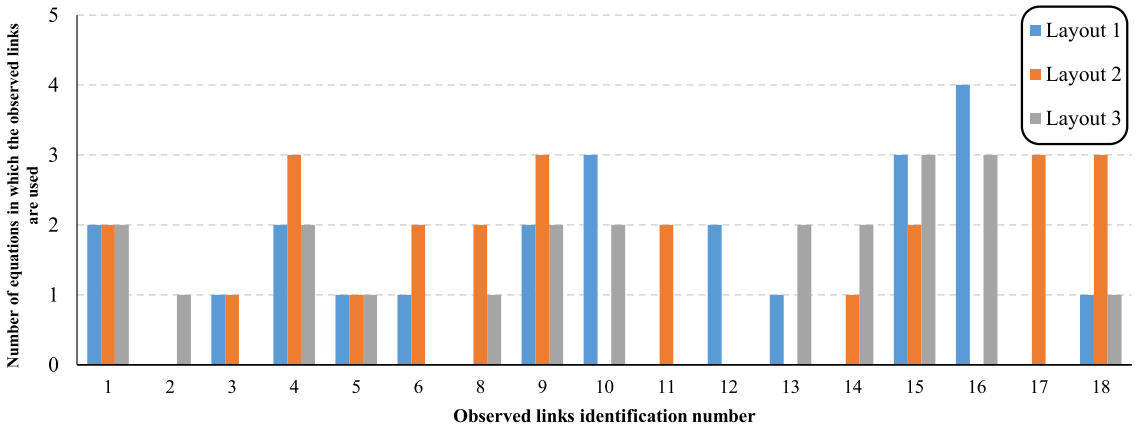

Fig. 7. The number of unobserved links requiring each observed link for their link flow inference.

Table 7
Sensor deployment in the Fishbone network for three different budget caps.

Budget (×100$)	Set of observed links equipped with sensors		OF[a]	No. of appearance of observed links in separate equations																	
	Type 1	Type 2		1	2	3	4	5	6	7	8	9	10	11	12	13	14	15	16	17	18
1500	{1, 3, 4, 7, 8, 9, 10, 13, 14, 15, 18}	{16}	5.38	2	–	1	2	–	–	1	1	2	2	–	–	2	2	3	3	–	1
1700	{1, 2, 4, 5, 8, 9, 12, 14}	{10, 16, 17, 18}	5.08	2	1	–	2	1	–	–	1	2	3	–	2	–	1	–	2	3	3
2000	{3, 13, 14, 17}	{1, 4, 5, 6, 9, 10, 15, 16}	4.70	2	–	1	2	1	1	–	–	2	2	–	–	2	2	3	3	1	–

[a] OF stands for objective function and it represents the expected number of unobserved links whose flow cannot be inferred due to the failure of sensors

link 16 appears in four different equations which is the highest number of appearances among other observed links in the first layout. In the case of the second layout, observed links 4, 9, and 17 exist in three different equations used for the link flow inference of unobserved links. For the third layout, the highest number of appearances of an observed link cannot exceed the analogous value for an observed link obtained in the second layout, as it is defined as a constraint for this layout. In this layout, the failure of observed links 15 and 16 can have the highest impact on the link flow inference of unobserved links as they appear in three equations. In Fig. 7, if there is no bar related to a layout for a given link in the horizontal axis of this figure, then it conveys that this link is not an observed link in that layout. For instance, there is no blue or orange bar for link 2 in Fig. 7, which means that link 2 is not an observed link in layouts 1 and 2.

Table 7 presents the location of sensors in the Fishbone network and the type of sensors to be installed in these locations for three different budgets using the min-sum objective function. In this table, we defined three different budgets of 1500$, 1700$, and 2000$. We assumed that the model shouldn't install more sensors (i.e., more than 12 sensors) as the budget increases, but rather allow the employment of more advanced sensors in the network. This is a valid assumption considering the significant installation cost of sensors in a network. We also assumed the heavy vehicle traffic loads are not high enough to affect the sensors' performance. According to this table, as the budget cap increases, the expected number of unobserved links whose flow cannot be inferred due to the failure of sensors decreases because the model can install more advanced sensors (i.e., sensors with lower failure probability) in the network. For instance, when the budget increases from 1500$ to 2000$, the number of links instrumented with sensor type 2 increases from only one link to eight links. Table 7 also compares the relationship between the types of sensor installed on an observed link with the number of appearances of that link in equations used for the link flow inference of unobserved links. According to this comparison, the model tends to install type 2 sensors on the observed links with a higher rate of appearance in different equations in order to minimize the expected number of unobserved links where their flow cannot be inferred due to the failure of a sensor. For instance, when the budget cap is set as 1700$, links 10, 17, and 18, which appear for the link flow inference of three unobserved links, i.e., are present in three different equations, are instrumented with sensor type 2. All links equipped with sensor type 1 have appeared in the link flow inference equations for the maximum of two unobserved links. Note that the results provided in Table 7 employing the proposed GA algorithm are obtained in 5–9 s.

9.2. Full link flow observability considering major roads: Sioux Falls network

We investigated the effect of considering major roads on the sensor positioning to reach full link flow observability in the Sioux Falls network. The right side of Fig. 8 provides a map of the Sioux Falls network. This network is surrounded by highway 90 at the top, and highways 29 and 229 on the left and right sides, respectively. These highways are red-colored, so they can be easily distinguished from the minor roads in the network. We considered these highways as the major roads in this network and assigned a higher weight to them. The left side of Fig. 8 demonstrates the graphical illustration of this

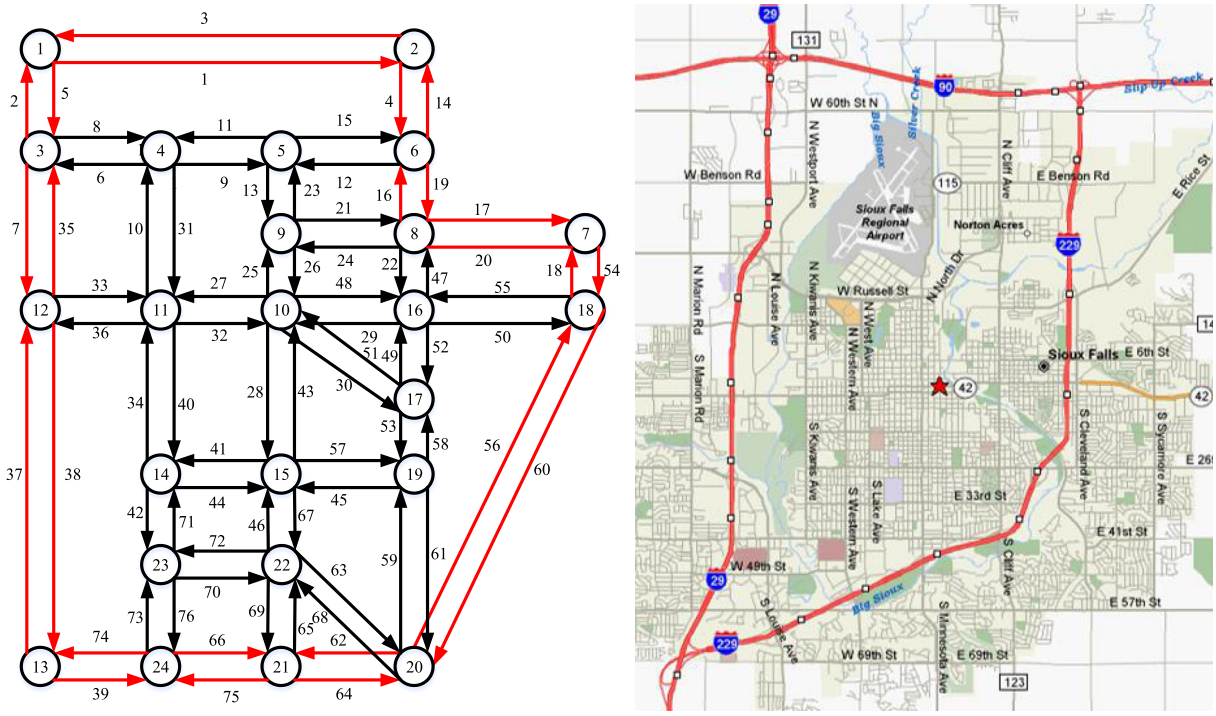

Fig. 8. Graphical illustration of the Sioux Falls network.

network and employs a color coding analogous to the right side of the figure to differentiate the major from the minor roads. Moreover, similar to Xu et al. (2016), we did not specify centroid nodes for the Sioux Falls network. This omission of centroid nodes can be justified by long-term counting as indicated by Ng (2013). Ng (2013) argued that centroid nodes can be ignored when traffic count information is collected over an entire day since the origin and destination nodes are interchangeable in the case of daily counts. In other words, a person who leaves home to go to work will return home later. According to this assumption, there are 24 non-centroid nodes in the Sioux Falls network, as well as 76 links which connect these non-centroid nodes. We provide a table that includes the sets of new links associated with the Sioux Falls network in Appendix III. According to Appendix III, out of 24 non-centroid nodes, 23 have non-empty sets of new links, and based on the instruction provided in the concept of new links, from each non-empty set of new links, one link should be selected as an unobserved link. This means that 23 out of 76 links are selected to not be equipped with sensors in the Sioux Falls network and that the rest of the links should be instrumented with sensors.

To begin with, we construct the set of initial solutions using the original sets of new links using Eq. (25) as the objective function and Eqs. (18-21) as the constraints, while the weight value of major roads is set as 1 and the rest of the roads are given a weight of 0.5. Table 8 shows the original sets of new links associated with the non-centroid nodes of the Sioux Falls network. Note that the results using this approach are presented under "*Scenario 1*".

Considering manual assignment of sensors to major roads, we updated the set of new links under two different scenarios named "*Scenario 2*" and "*Scenario 3*". In Scenario 2, we removed the links in the set of major roads from each set of new links and assigned sensors to these links (Please see the column labeled Scenario 2 in Table 8). This elimination of major roads results in seven sets out of 23 sets of new links becoming empty sets. Therefore, to construct the set of unobserved links, we need to select more than one link from some of the sets of new links which could result in the matrix of unobserved links becoming a singular matrix. To avoid the creation of a singular matrix, the non-zero determinant condition for the matrix of unobserved links enforced in Eq. (24) needs to be satisfied. Note that in applying Scenario 2, we ran the proposed GA to generate the initial population, but the GA didn't manage to reach any feasible solution in which the matrix of unobserved links is invertible. This outcome occurred despite using different sizes for the initial population and a considerable number of attempts[8] to generate the initial population, up to 10^5attempts.

According to Scenario 3, we attempted to remove the major roads from the sets of new links in a way to avoid these sets becoming empty sets (Please see the column labeled Scenario 3 under 'Updated sets of new links' in Table 8). Therefore, under this scenario, we can still use the concept of new links to generate feasible solutions. Using the updated sets of new links in Scenario 3, we could select up to 17 links from the set of major roads to be instrumented with sensors in initial

[8] The phrase "number of attempts" refers to the number of times the GA attempted to generate the initial population.

Table 8
Original and updated sets of new links related to the Sioux Falls network.

Node	Connected links	Sets of new links	Updated sets of new links		Major roads removed from the sets of new links	
		Scenario 1	*Scenario 2*	*Scenario 3*	*Scenario 2*	*Scenario 3*
1	1,2,3,5	{1, 2, 3, 5}	–	{1}	1,2,3,5	2,3,5
2	1,3,4,14	{4, 14}	–	{4}	4,14	14
3	2,5,6,7,8,35	{6, 7, 8, 35}	{6, 8}	{6, 8}	7,35	7,35
4	6,8,9,10,11,31	{9, 10, 11, 31}	{9, 10, 11, 31}	{9, 10, 11, 31}	–	–
5	9,11,12,13,15,23	{12, 13, 15, 23}	{12, 13, 15, 23}	{12, 13, 15, 23}	–	–
6	4,12,14,15,16,19	{16, 19}	–	{16}	16,19	19
7	17,18,20,54	{17, 18, 20, 54}	–	{17}	17,18,20,54	18,20,54
8	16,17,19,20,21,22,24,47	{21, 22, 24, 47}	{21, 22, 24, 47}	{21, 22, 24, 47}	–	–
9	13,21,23,24,25,26	{25, 26}	{25, 26}	{25, 26}	–	–
10	25,26,27,28,29,30,32,43,48,51	{27, 28, 29, 30, 32, 43, 48, 51}	{27, 28, 29, 30, 32, 43, 48, 51}	{27, 28, 29, 30, 32, 43, 48, 51}	–	–
11	10,27,31,32,33,34,36,40	{33, 34, 36, 40}	{33, 34, 36, 40}	{33, 34, 36, 40}	–	–
12	7,33,35,36,37,38	{37, 38}	–	{37}	37,38	38
13	37,38,39,74	{39, 74}	–	{39}	39,74	74
14	34,40,41,42,44,71	{41, 42, 44, 71}	{41, 42, 44, 71}	{41, 42, 44, 71}	–	–
15	28,41,43,44,45,46,57,67	{45, 46, 57, 67}	{45, 46, 57, 67}	{45, 46, 57, 67}	–	–
16	22,29,47,48,49,50,52,55	{49, 50, 52, 55}	{49, 50, 52, 55}	{49, 50, 52, 55}	–	–
17	30,49,51,52,53,58	{53, 58}	{53, 58}	{53, 58}	–	–
18	18,50,54,55,56,60	{56, 60}	–	{56}	56,60	60
19	45,53,57,58,59,61	{59, 61}	{59, 61}	{59, 61}	–	–
20	56,59,60,61,62,63,64,68	{62, 63, 64, 68}	{63, 68}	{63, 68}	62,64	62,64
21	62,64,65,66,69,75	{65, 66, 69, 75}	{65, 69}	{65, 69}	66,75	66,75
22	46,63,65,67,68,69,70,72	{70, 72}	{70, 72}	{70, 72}	–	–
23	42,70,71,72,73,76	{73, 76}	{73, 76}	{70, 72}	–	–
24	39,66,74,75	–	–	–		

solutions (Please see the last column labeled Scenario 3 in Table 8). However, the number of major links to be equipped with sensors can increase in the subsequent feasible solutions generated by the GA. We then employed the objective function and the constraints introduced in Section 5.2 to minimize the expected number of unobserved links whose flow cannot be inferred due to the failure of sensors. Note that for all scenarios, we assumed that the budget is enough to afford 24 sensors of type 2 and 29 sensors of type 1.

Fig. 9 demonstrates the objective function value, i.e., Eq. (25), using the proposed GA under Scenarios 1 and 3 in 1410 iterations. For each scenario, we defined three different initial populations with distinctive population sizes. Fig. 9 shows that both scenarios converge to nearly similar results, while the larger population sizes perform slightly better in minimizing the objective function.

To investigate the effect of considering major roads on the layout of sensors, we used Eqs. (17) and (25) as the objective functions to observe the possible differences in suggested layouts of sensors in the Sioux Falls network. Fig. 10 illustrates two optimum layouts of sensors in this network using different objective functions. In layout A, the objective function is as Eq. (17) to minimize the expected number of unobserved links where their flow cannot be inferred due to the failure of sensors. In layout B, a similar goal is pursued using Eq. (25) but also incorporates the relative importance of major roads in finding the location of sensors while using the original sets of new links to generate initial solutions. Fig. 10 demonstrates that in layout B, the GA assigns more advanced sensors, i.e., sensors with a lower probability of failure, to the major roads. It also minimizes the number of major roads to be included in the set of unobserved links. The reason for this minimization is due to the fact that the probability of missing the link flow inference of an unobserved link is usually higher than the probability of missing the link flow observation of that link as an observed link if more than one link is required for the link flow inference of that link. Note that the results of sensor deployment depicted in Fig. 10 by employing the proposed GA are achieved in 15–25 s.

Fig. 11 evaluates the number of major links equipped with sensor type 2, i.e., advanced sensor, for the suggested layouts using Eqs. (17) and (25) in each iteration of GA. The initial populations with respect to major roads are generated under Scenarios 1 and 3. In initial populations, 7 links (Scenario 1) and 17 links (Scenario 2) from the set of major roads are instrumented with the sensor type 2. However, the number of links equipped with sensor type 2 converges to the same value under these scenarios as the iterations proceed. According to this figure, through 1410 iterations, the layouts provided by the consideration of major roads using Eq. (25) attempt to assign on average more sensors of type 2 to the major roads. For instance, for the last 900 iterations, out of 24 major roads in the Sioux Falls network, on average 20 links are instrumented with sensor type 2 using Eq. (25) for both Scenarios 1 and 3, while this average drops to 16 links when the concept of major roads is not applied.

Fig. 12 shows the number of major roads to become unobserved links in layouts generated by the proposed GA under Scenarios 1 and 3 with either the consideration of major roads or not. According to this figure, the number of major roads

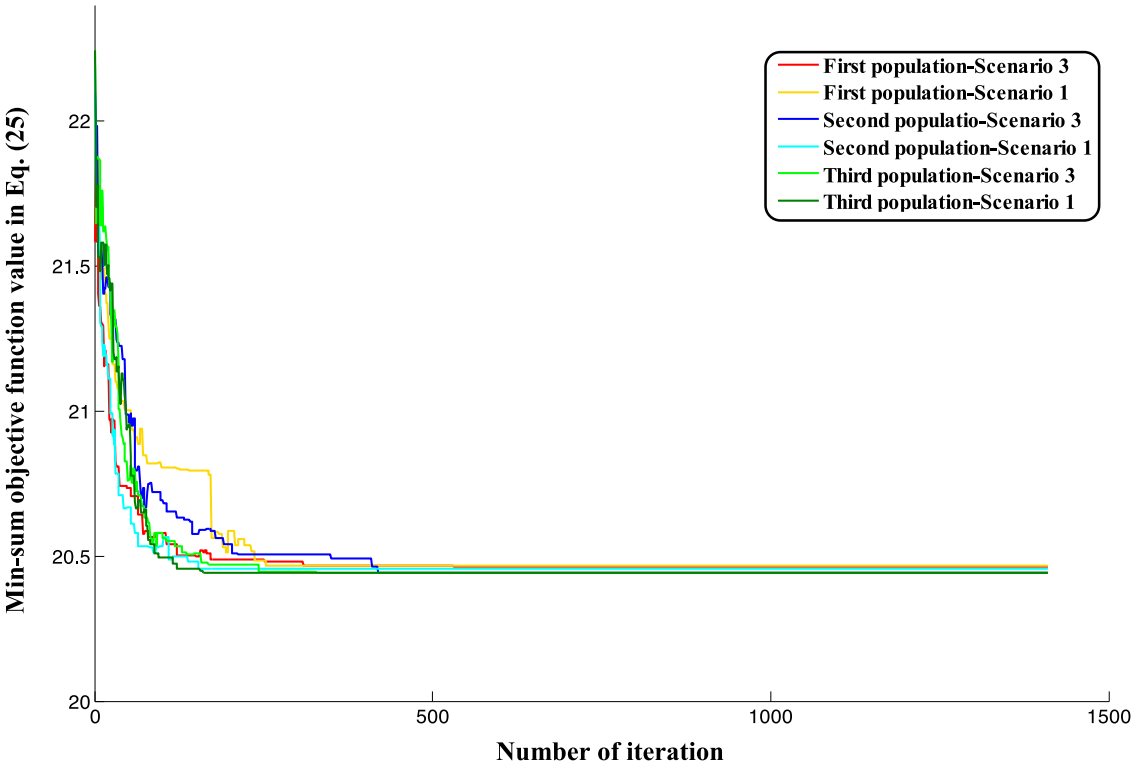

Fig. 9. Results of implementing Scenarios 1 and 3 with different populations for the Sioux Falls network.

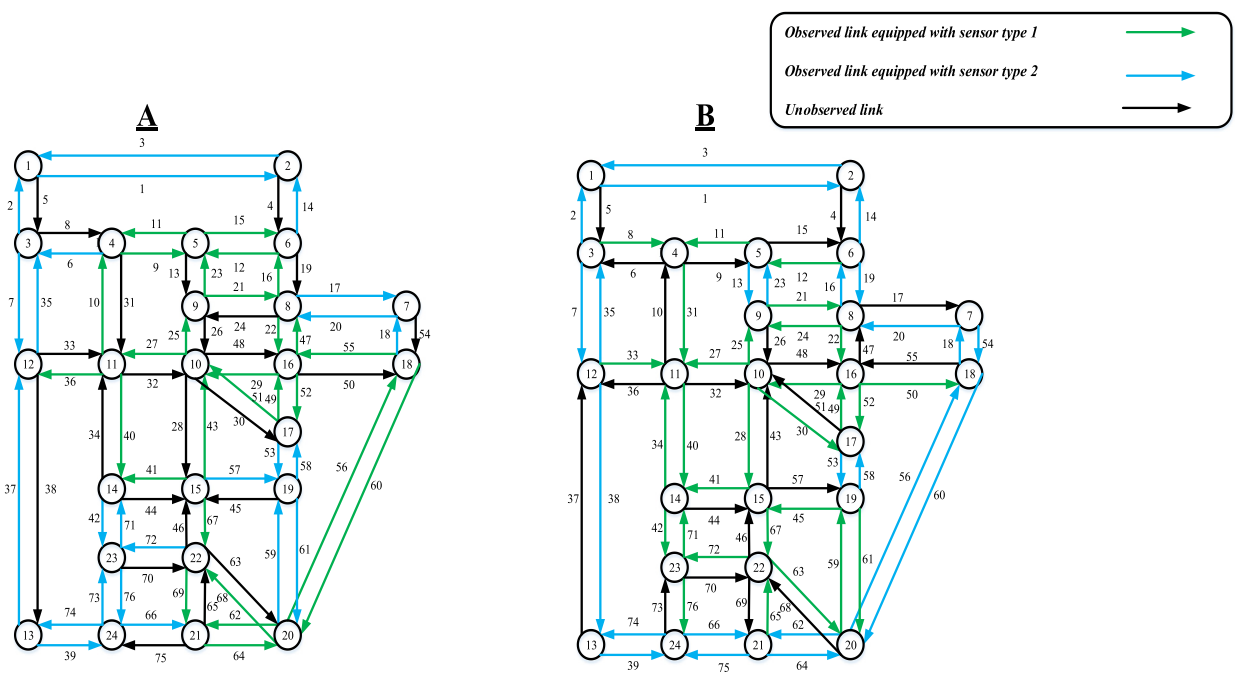

Fig. 10. Two optimum layouts of sensors with and without consideration of major roads.

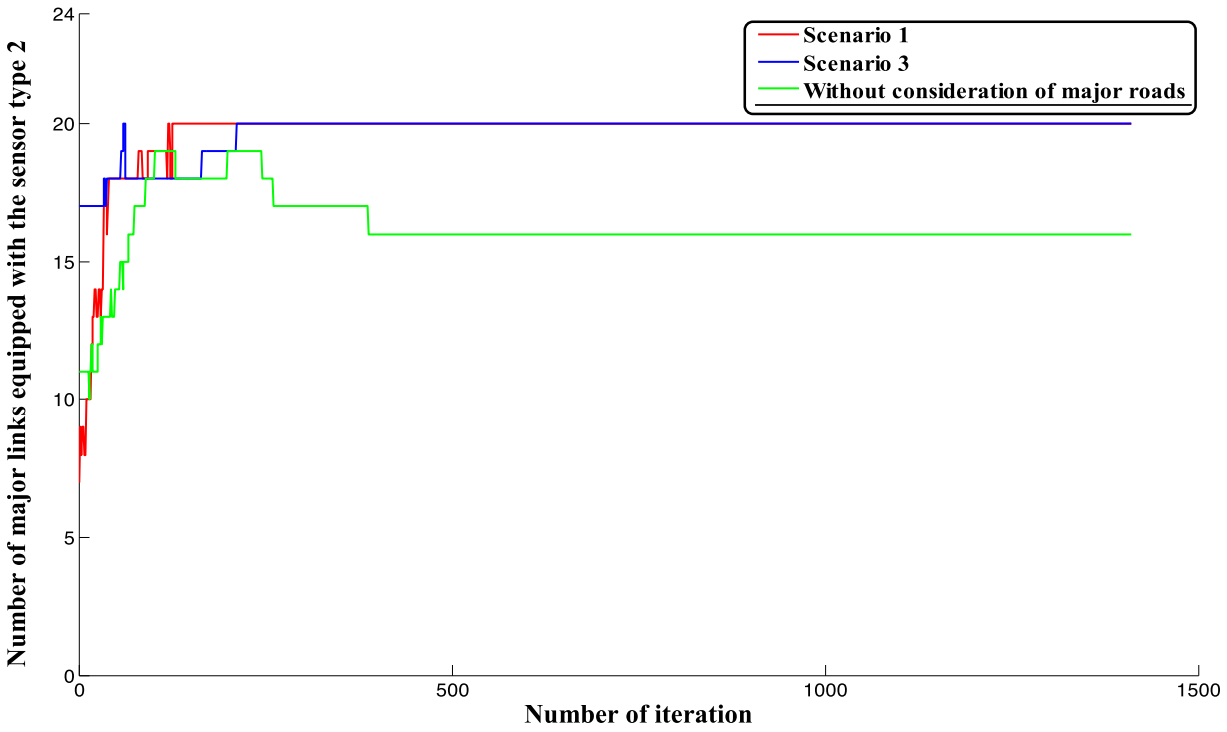

Fig. 11. Number of major links instrumented with sensor type 2 in Sioux Falls network.

Table 9
Sensor deployment considering major links with and without high HVL in Sioux Falls network.

Layout	Observed links				Unobserved links	
	Major links and HVL > 3.5% TL		HVL > 3.5% TL		Major links and HVL > 3.5% TL	HVL > 3.5% TL
	Type 1	Type 2	Type 1	Type 2		
B	0	6	8	0	2	4
C	0	7	3	4	1	5

included in the set of unobserved links when the major links are considered is 25% lower in the last 800 iterations compared to the situation when all links are assumed to be identical.

9.3. Full link flow observability considering major roads and heavy vehicle loads: Sioux Falls network

To assess the effect of considering major roads on the layout of sensors, we implemented the proposed model in the Sioux Falls network using Eq. (25) as the objective functions as well as the updated probability of failure of sensors under high load of heavy vehicles introduced in Table 5. We considered the roads going to the depot areas located in the northwest and southwest sections of Sioux Falls as the roads with high HVL (i.e., HVL > 3.5% TL). Fig. 13 illustrates the optimum layout of sensors, introduced as layout C, in this network using 24 sensors of type 2 and 29 sensors of type 1. This combination of sensors is similar to the one we used in Section 9.2. In Fig. 13, there are 20 links under high loads of heavy vehicles, indicated by the red double backslashes. In the layout shown, more than 50% of links (i.e., 11 links) with high HVL are equipped with the sensor type 2 and in general, 70% of links (14 links) with high HVL are instrumented with sensors.

Table 9 evaluates the effect of considering the high HVL on sensor positioning in the Sioux Falls network. In this table, layout B (introduced in Fig. 10) only considers the major roads, while layout C (depicted in Fig. 13) considers both the major roads and roads with high HVL (i.e., HVL > 3.5% TL) in the Sioux Falls network. Comparing observed links in layouts B and C in Table 9, we see there is a 16.7% increase in deployment of sensor type 2 on the major links with high HVL in layout C. This means that in considering the effect of HVL on sensor failure, the proposed model attempts to install more advanced sensors on the major links which are also subject to high HVL, in an effort to decrease the adverse effect of high HVL on the link flow observability of observed links and on the link flow inference of unobserved links. Moreover, there is a considerable increase (i.e., 50%) in the number of sensor type 2 deployed on non-major links with high HVL in layout C compared to layout B. This increase indicates that the model makes a similar effort to instrument links with high HVL with more advanced sensors when these links are not among major links. Eventually, exploring unobserved links in each

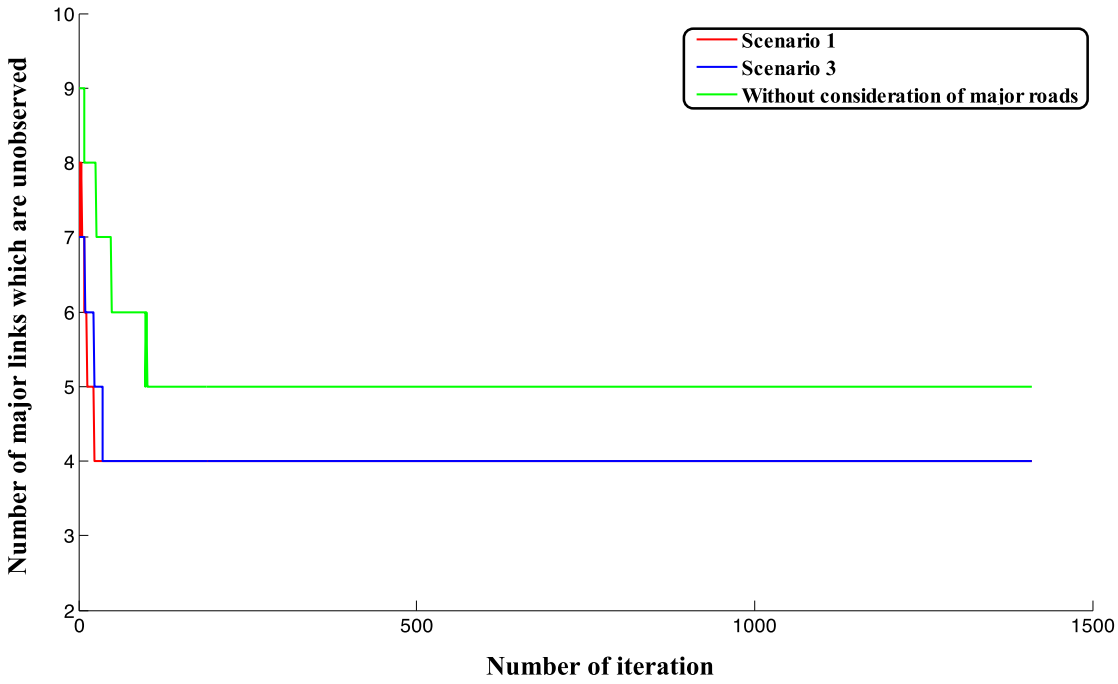

Fig. 12. Number of major links to be included in the set of unobserved links.

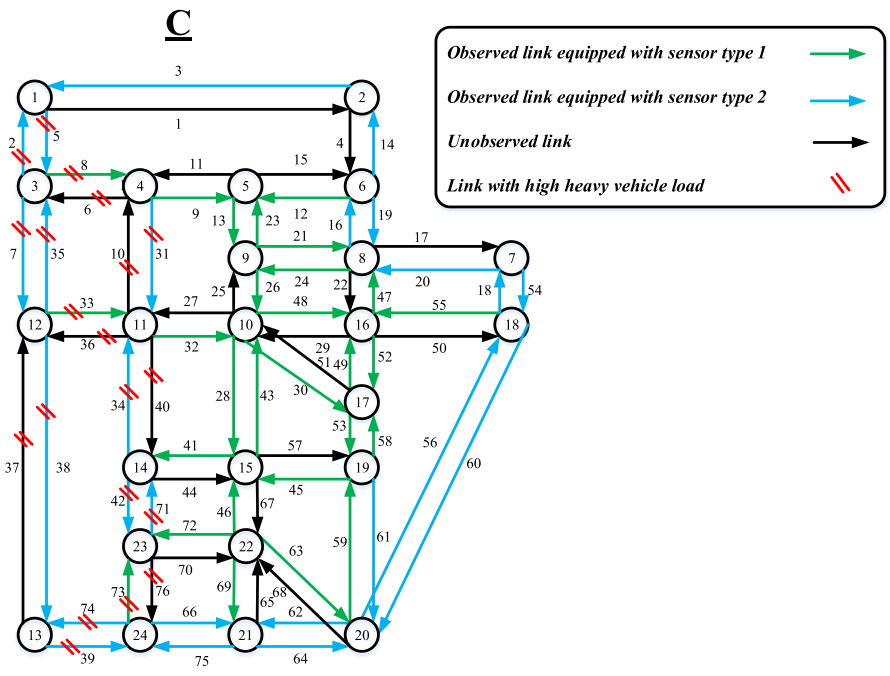

Fig. 13. Optimum layout of sensors with consideration of major roads and heavy vehicle loads.

layout, we found that the number of unobserved links from the set of major links with high HVL decreases in layout C. This is due to the fact that the probability of missing the link flow inference of an unobserved link is usually higher than the probability of missing the flow observation of an observed link; therefore, the proposed model attempts to minimize the number of major links with high HVL in the set of unobserved links. Note that the runtime for achieving the results presented in Table 9 is 17 to 19 s depending on the size of the initial population for the Sioux Falls network in the proposed algorithm.

Fig. 14. The Irvine network.

9.4. Full link flow observability in large networks: Irvine network

In this section, we evaluated the performance of the proposed model for a relatively large network. To do so, we selected the Irvine network which is graphically demonstrated in Fig. 14. The major roads, which mainly comprise the north-south and east-west bound highways, are highlighted in red in the figure. The extracted network consists of 162 non-centroid nodes, 496 links, 39 traffic analysis zones (TAZs), and 28 external stations, i.e., there are 67 centroid nodes (28+39).[9] In Fig. 14, 112 out of 496 links are marked as major roads.

For the Irvine network, we compared the results of implementing the proposed model to the results obtained by Xu et al. (2016). Xu et al. (2016) reduced the flow variance measurement of unobserved links by minimizing the number of observed links required for flow variance measurement of each unobserved link. They used a genuine approach to tackle the problem, attempting to minimize the number of unobserved links connected to each non-centroid node in order to minimize the number of observed links required for flow variance measurement of each unobserved link. As the number of observed links required for variance measurement of unobserved links can be also employed to infer the flow of unobserved links, Xu et al. (2016) approach, despite its differences, can be compared to the model proposed in this work. However, to make a comparison, we need to assume that all sensors are identical and that there is no major road in the network. Fig. 15 shows the average number of observed links required to infer the flow of unobserved links, i.e., Eq. (10). According to the algorithm procedure explained in Section 8, we implemented the proposed model with three different population sizes and

[9] These data were extracted from the Orange County Transportation Analysis Model.

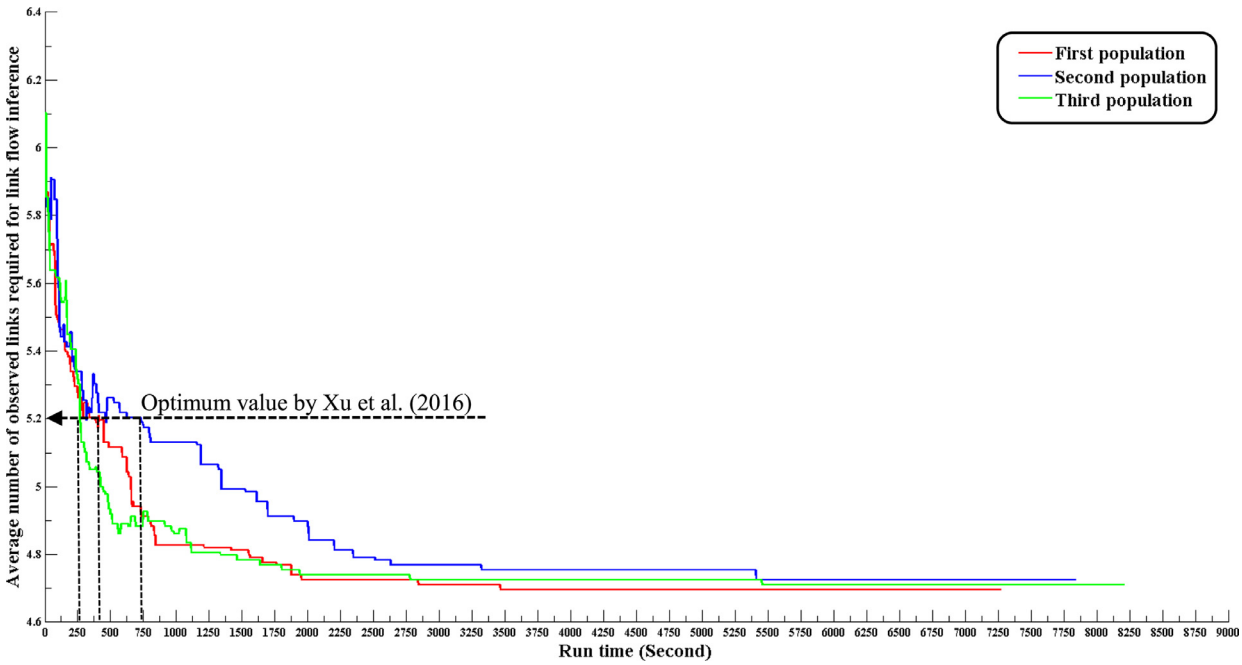

Fig. 15. Results of implementing the proposed model with Eq. (10) as the objective function in the Irvine network.

Table 10
Number of unobserved links connected to each non-centroid node.

Model	Objective function	# of unobserved links connected to non-centroid node(s)			
		One	Two	Three	Four
Xu et al. (2016)	Min-max	64	78	20	0
	Min-sum	86	56	19	1
Proposed model	Eq. (10)	113	23	22	4

9136 iterations.[10] The horizontal axis in Fig. 15 depicts the runtime in seconds. According to this figure, the maximum time it takes to reach the optimum value i.e., minimum of the average number of observed links needed to infer the flow of each unobserved link, among all populations is 8207 s (2.27 h). In Fig. 15, we also marked the time it takes the proposed model to reach the optimum value of Eq. (10) obtained by Xu et al. (2016). According to Fig. 15, the maximum time it takes the proposed model to reach this value is 750 s. In comparison with Xu et al. (2016) work, the proposed model can successfully decrease the average number of observed links required to infer the flow of unobserved links, although, we were not able to compare the runtime with Xu et al. (2016) as it was not reported in their work.

Table 10 shows some of the potential differences in sensor positioning in the Irvine network using the proposed model and the model developed by Xu et al. (2016). This table indicates the number of unobserved links connected to each non-centroid node in the Irvine network for both Xu et al. (2016) and the proposed model. As presented in Table 10, Xu et al. (2016) used two objective functions, the min-max and min-sum functions. Their min-sum objective function attempts to minimize the summation of the number of unobserved links connected to each non-centroid node and their min-max function minimizes the maximum number of unobserved links connected to a non-centroid node. Considering the number of unobserved links connected to each non-centroid node, we can observe that compared to Xu et al. (2016), the proposed model increases the number of non-centroid nodes connected to only one unobserved link. In addition, the number of non-centroid nodes linked to four unobserved links is considerably larger in the results associated with the proposed model. This analysis leads us to the conclusion that the objective functions introduced in Xu et al. (2016) can be modified to focus only on the non-centroid nodes connected to one unobserved link instead of all non-centroid nodes which may attach to more than one unobserved link.

In Table 11, we implemented the proposed model in the Irvine network, considering three different sensor assignment scenarios for major roads in the network. In the first scenario, we assigned weights to links and solved the model employing Eq. (25). On the other hand, in the second and third scenarios, similar to what we implemented in Table 8 for the Sioux Falls network, we tried to manually assign advanced sensors in the initial population of the proposed GA. Similar to the results

[10] The number of iterations was obtained according to the method outlined in Section 9.1.

Table 11
Sensor installation in the Irvine network considering major roads.

Scenario	# of major links			Runtime
	Observed links		Unobserved links	
	Type 1	Type 2		
Scenario 1	7	92	13	7460
Scenario 3				7133

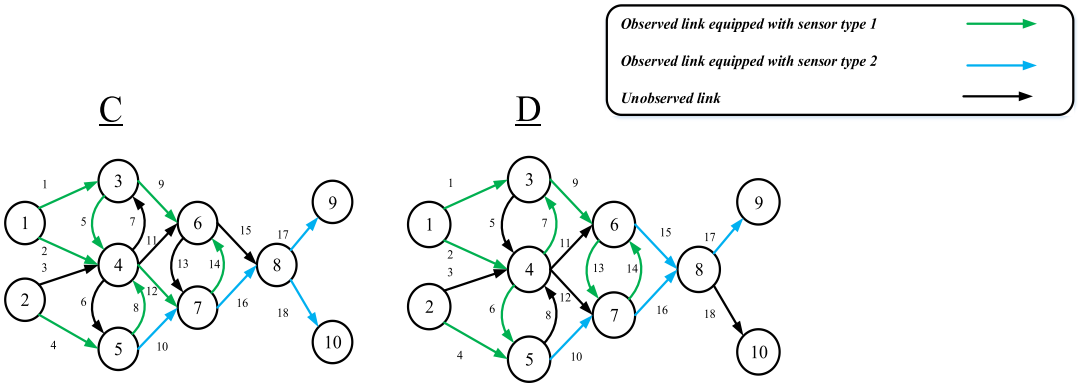

Fig. 16. Two optimum layouts of sensors in Fishbone network.

obtained for the Sioux Falls network, we could not generate a feasible initial population using Scenario 2. However, we can successfully implement Scenarios 1 and 3 and the results are presented in Table 11. As shown in Table 11, out of 112 major links, 92 (82.1%) are equipped with a more advanced sensor, i.e., sensor type 2, and only 11.6% of all major links are in the set of unobserved links. Comparing the runtime for Scenarios 1 and 3, we observed that the manual assignment of sensors, while not very practical for large networks, could lead to lower runtime. The reason behind the reduction in runtime under Scenario 3 may relate to the higher number of major links equipped with more advanced sensors in the initial population of Scenario 3 compared to Scenario 1, which facilitates the convergence speed to the optimum solution.

9.5. Full link flow observability with route flow information: Fishbone network

In Section 6, we suggested a two-level optimization model to consider the effect of route flow information on the assessment of sensor layouts which lead to full link flow observability. According to Section 6, the optimum solutions for full link flow observability should be obtained in the first level optimization. The second level optimization then minimizes the information loss from all routes that provide unique information about route flows, while guaranteeing full link flow observability and not worsening the objective function value reached in the first level optimization. In this section, we used the Fishbone network to showcase how the two-level optimization model can be implemented, while setting the budget cap as 1700 and assuming the load of heavy vehicles is less than 3.5% of total traffic load. Following the budget constraint and HVL assumption, Table 7 demonstrates only one of the possible optimum layouts of sensors in the Fishbone network. We reapplied the proposed model to find one other possible optimum layout of sensors which results in the same objective function value. Fig. 16 depicts two optimum sensors layouts in the Fishbone network in which green and blue arrows represent the links equipped with sensor types 1 and 2, respectively. In this figure, layout C is the sensor layout introduced in Table 7 and layout D is another possible layout of sensors, with the objective function value for both layouts equal to 5.08. Note that for the Fishbone network, the number of possible optimum layouts which constitute the pool of feasible solutions in the second level optimization was more than two. However, we displayed only two possible layouts to easily describe the procedure for finding the sensor layouts that not only minimize the effect of sensor failure on link flow inference of unobserved links, but also minimize the effect of sensor failure on route flow information gain.

Table 12 represents four ODs and eight identified routes[11] between these ODs in the Fishbone network. All of these routes belong to sets R^2 and $R^{3'}$ introduced in Section 6. Routes 1, 5 and 8 belong to R^2 as the set of links {9}, {6, 10}and {4, 8}are only traversed by these routes, respectively, while the other routes belong to $R^{3'}$. All of these routes can contribute to information gain, as the column vectors pertaining to these routes in the link-route incidence matrix are linearly independent. Table 12 also presents the links traversed by each route and instrumented with sensors in layout C or D. The last column of the table shows the probability of missing the route flow observability of each route if sensor positioning

[11] For simplicity, in Table 12 we introduce only some of all the possible routes between each OD as the set of identified routes.

Table 12
Identified routes between each OD and links traversed by these routes in the Fishbone network.

OD	Set of involved links in each route	Set of observed links in each layout				Possibility of missing route flow observability	
		C		D		C	D
		Type 1	Type 2	Type 1	Type 2		
1–9	Route 1: {1, 9, 15, 17}	{1, 9}	{17}	{1, 9}	{15, 17}	0.075	0.0225
	Route 2: {2, 12, 14, 15, 17}	{2, 12, 14}	{17}	{2, 14}	{15, 17}	0.0375	0.0225
	Route 3: {1, 5, 11, 15, 17}	{1, 5}	{17}	{1}	{15, 17}	0.075	0.045
1–10	Route 4: {1, 5, 11, 15, 18}	{1, 5}	{18}	{1}	{15}	0.075	0.15
	Route 5: {2, 6, 10, 16, 18}	{2}	{10, 16, 18}	{2, 6}	{10, 16}	0.0135	0.0225
2–9	Route 6: {3, 11, 15, 17}	–	{17}	–	{15, 17}	0.5	0.09
	Route 7: {3, 12, 14, 15, 17}	{12, 14}	{17}	{14}	{15, 17}	0.075	0.045
2–10	Route 8: {4, 8, 12, 16, 18}	{4, 8, 12}	{16, 18}	{4}	{16}	0.01125	0.15
					Σ	0.86225	0.5475

follows layout C or D. For instance, route 4 traverses links 1, 5, 11, 15, and 18. Among these links, the set of links {1, 5, 18} and {1, 15} are equipped with sensors in layouts C and D, respectively. The probability of missing the route flow observability of route 4 depends on the *number of sensor-instrumented links traversed by this route* as well as *the sensor type* installed on these sensor-equipped links. In layout C, as both links 1 and 5 are equipped with sensor type 1, and link 18 is instrumented with sensor type 2, then the probability of missing the route flow observability of route 4 equals 0.075[12] ($0.5^2 \times 0.3 = 0.075$). In layout D, this probability equals 0.15, as links 1 and 15 are instrumented with sensor types 1 and 2, respectively ($0.5 \times 0.3 = 0.15$). Adding the probability of missing the route flow observability of all routes in layouts C and D, we can obtain the objective function value of the second level optimization introduced in Eq. (31). By doing so, we observe that although having the same objective function value in the first level, the objective function for layouts C and D differs in the second level of the two-level optimization model. In fact, the expected number of routes for which flow will be missed due to the failure of sensors in layout C equals 0.86225, and is higher than the similar expected value for layout D. This means layout D offers more robust sensor positioning compared to layout C if the link-route incidence matrix information is available.

9.6. Redundant sensors: Fishbone network

The concept of redundant sensors is mainly developed in this work to investigate the location of additional sensors in a network to maintain the full link flow observability when certain sensors already installed on observed links stop functioning. According to the stepwise approach introduced in Section 7, we first need to determine the initial location of sensors in a network to be able to consider the combination of failures among them in the second step. In the third step, the location of redundant sensors should be selected for each combination of failure. Finally, in the fourth step, taking into account budget constraints, the sensors are assigned to the locations identified in the third step.

To make it easier to demonstrate how the concept of redundant sensors can be applied to a network, we only consider the Fishbone network to be equipped with redundant sensors. The initial location of sensors is assumed to be according to the third layout determined in Table 7. We also assume that all the redundant sensors are identical and can be independently installed in a network.

Table 13 shows the set of observed links according to the third layout of Table 7 as well as the failure probability of the sensors installed on these links. This table also shows the location of redundant sensors while considering the failure of only one sensor among all sensors located on observed links. To obtain the location of redundant sensors, we used Eq. (17) but dropped the binary variable y_{fj} and the parameter p_f as we assumed all sensors are identical. In total, six links can be nominated for installing the redundant sensors, including links 2, 7, 8, 11, 12 and 18, as these links were not initially instrumented with sensors according to the third layout of Table 7.

Links suggested for installing redundant sensors in Table 13 are based on the assumption that out of twelve links instrumented with sensors, the sensor installed in only one of these links breaks down. The information provided in Table 13 can also be used to determine the expected number of times a link will be selected for installing the redundant sensors. For instance, link 18 is selected to be equipped with redundant sensors if the sensors installed in link 15, 16 or 17 stop working. The probabilities of failure of the sensors installed in these links are 0.3, 0.3, and 0.5, respectively. Therefore, the expected number of times that link 18 is selected to be instrumented with a redundant sensor is 1.1.

In line with the third step introduced in Section 7, Table 14 shows the set of links selected to be equipped with redundant sensors for different combination of failures. This tables also determines, for each combination of sensor failure, the percentage of links missing full link flow observability even with redundant sensors installed in the Fishbone network. For instance, considering a two sensor failure out of twelve installed sensors, we can observe that in one out of the 66 possible combinations of failure, the full link flow observability is impossible even with the installation of redundant sensors. This

[12] This probability is calculated assuming that heavy vehicle load (HVL) is less than 3.5% of total traffic load.

Table 13
Possible location of redundant sensors with only one sensor failure among all sensors installed on observed links.

Set of observed links	Sensor failure Link location	Probability	New observed link
{1, 3, 4, 5, 6, 9, 10, 13, 14, 15, 16, 17}	1	0.3	7
	3	0.5	2
	4	0.3	8
	5	0.3	7
	6	0.3	8
	9	0.3	7
	10	0.3	8
	13	0.5	12
	14	0.5	12
	15	0.3	18
	16	0.3	18
	17	0.5	18

Table 14
Results related to redundant sensors in the Fishbone network.

Combination of sensor failures	Total possible combinations	% missing full link observability	Set of links to be equipped with redundant sensors	Expected number of selections
One failure	$\binom{12}{1} = 12$	0%	{18}	1.1
Two failures	$\binom{12}{2} = 66$	$\frac{1}{66}$ (1.5%)	{7, 18},{8, 18}	0.99
Three failures	$\binom{12}{3} = 220$	$\frac{14}{220}$(6.4%)	{2, 7, 18},{2, 8, 18}	0.77
Four failures	$\binom{12}{4} = 495$	$\frac{82}{495}$(16.6%)	{2, 7, 8, 18}	0.74
Five failures	$\binom{12}{5} = 792$	$\frac{278}{792}$(35.1%)	{2, 7, 8, 12, 18}	0.67
Six failures	$\binom{12}{6} = 924$	$\frac{601}{924}$(65%)	{2, 7, 8, 11, 12, 18}	0.63

situation occurs when sensors installed on links 13 and 14 are assumed to break down and these links become unobserved links. As links 13 and 14 are bidirectional links, the column vector associated with these links is linearly dependent. Therefore, the corresponding matrix of unobserved links is not invertible and the system of linear equations for the link flow inference of unobserved links is not determined. Table 14 also indicates that as the number of failures increases, the chance of missing the full link flow observability increases correspondingly. According to the fourth column of Table 14, for a certain number of failures, there might be more than one set of links to be equipped with redundant sensors. For instance, when it is assumed that three of twelve sensors installed on observed links break down, then two sets of links, including sets {2, 7, 18} and {2, 8, 18}, have the equal chance of being selected as the set of links to be instrumented with redundant sensors. The last column of Table 14 demonstrates the expected number of times each set of links will be selected.

In addition to finding the expected number of selections for each set of links to be equipped with redundant sensors in Table 14, we show the expected number of selections for individual links considering different combinations of failure in Fig. 17.

In Fig. 17, we show the expected number of selections for links, including links 2, 7, 8, 11, 12 and 18, to be instrumented with redundant sensors considering different combinations of failure. The horizontal axis of this figure shows different combinations of failure and the vertical axis represents the expected number of selections associated with each individual link. For instance, according to Table 14, in the case of two failures, each of sets {7, 18} and {8, 18} have the highest expected number of selections, .i.e., 0.99, compared to other sets to be instrumented with redundant sensors. For individual links, the expected number of selections of link 18 is 5.995 and the highest among other links in the case of two failures. The difference in this expected number of selections can be explained by the fact that link 18 might be available in other sets with an expected number of selections that is not as high as it is for sets {7, 18} and {8, 18}. Therefore, the last column of Table 13 does not count the total number of times that link 18 is selected to be equipped with redundant sensors except for the cases when one failure or six failures occur. In these cases, the expected frequency of selection in Fig. 17 and in the last column of Table 14 match as they include only one link (i.e., in case of one failure) or all links (i.e., in the case of six failures) that can be instrumented with redundant sensors.

According to Fig. 17, link 18 has the highest expected number of selections in each combination of failure. Therefore, according to the fourth step introduced in Section 7, if budget constraints allow, link 18 should be the first link to be equipped with redundant sensors. Links 8 and 7 stand in the second and the third ranks, respectively when comparing

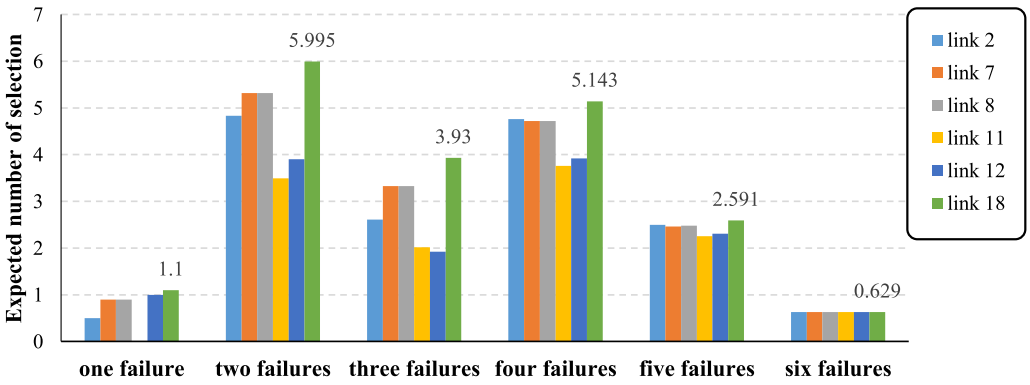

Fig. 17. Expected number of times a link is selected to be instrumented with sensors.

the total expected number of selections for all combinations of failure. Note that the expected frequency of selection for a certain link through the different combination of failures represents an irregular pattern, i.e., increasing or decreasing pattern, as it depends on the location of initial sensors, the number of failed sensors, as well as their probability of sensor failure.

10. Discussion on the effectiveness of the proposed model for partial link flow observability

Full link flow observability can be considered as the *ideal* case for link flow observability in a network as the flow of all links of that network can be directly observed or indirectly inferred. However, in the real world, it might not be economically possible to install enough sensors to reach full link flow observability. Instead, the partial link flow observability problem addresses the situation where there is a smaller number of sensors than the number required to reach full link flow observability. Researchers have introduced various definitions of partial flow observability and more specifically, the partial link flow observability in a network (Viti et al., 2014). Castillo et al. (2011) defined the partial link flow observability problem as the problem of finding a subset of links in a network that should be equipped with sensors in order to make it possible to infer the link flow of a certain number of unobserved links. For instance, in the Fishbone network, the number of unobserved links equals six. A problem which attempts to find the location of sensors in a way to infer the flow of five or a smaller number of unobserved links, is a partial link flow observability problem. Gentili and Mirchandani (2012) defined the number of unobserved links for which flow can be inferred using the information obtained from observed links as h, and indicated that partial link flow observability can be studied under different values of h, i.e., different levels of observability. There are other studies that address partial link flow observability when there is a given number of sensors (He, 2013; Ng, 2012). Moreover, to tackle the partial link flow observability problem from a different perspective, Hu et al. (2009) and Ng (2013) address the problem of finding the minimum number of sensors required to reach full link observability when there are already some sensors installed in a network. Concerning the definition proposed by Gentili and Mirchandani (2012), we can also address partial link flow observability using the proposed model. Specifically, as we studied the full link flow observability problem in a network considering the possible failure of sensors, our focus was to minimize the chance of decrease in the level of h if sensor failure occurs. For instance, Eq. (17) defined in Section 5 minimizes the effect of a sensor failure on link flow inference of unobserved links. In other words, this objective function attempts to assign more advanced sensors on links which appear in more equations required for link flow inference of unobserved links. Accordingly, the chance of reduction in the value of h decreases as more advanced sensors, which have lower failure rates, are installed on links with a higher appearance in equations used for link flow inference of unobserved links. For illustration, we selected the sensor location in the Fishbone network associated with layout C introduced in Fig. 16, to illustrate the possible decrease in the level of h if the sensor installed on an observed link stops functioning. According to Fig. 18, the failure of sensors installed on links 10, 16, 17 and 18 could have the highest impact on the level of observability as their failure can decrease the level of observability from $h=6$ to $h=3$. As we can observe in Fig. 18, the model assigned more advanced sensors (i.e., sensor type 2) on these links to minimize the adverse effect of sensor failure on the level of observability.

From a different perspective, the partial link flow observability concerns maximizing the *observability level* for a given number of sensors. Using the proposed model, we can still maximize the observability level, but also minimize the adverse effect of sensor failure on link flow inference of unobserved links. The concept of new links can help us to determine the number of sensors required to reach full link flow observability in a network. Specifically, using the concept of new link, we can determine the number of sensor deficiencies that leads to not enough sensors to reach full link flow observability in a network. As our proposed model is designed to guarantee full link flow observability using an adequate number of sensors, we can adjust the deficiency in the number of sensors required to reach full link observability in a network with some *buffer sensors* that have a failure probability of $1-\varepsilon$ where ε is a very small value. Buffer sensors are not *available sensors* but they

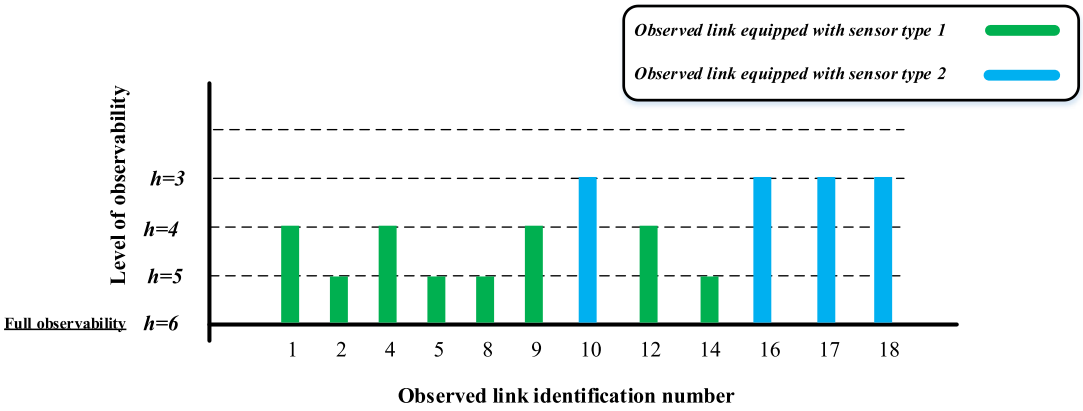

Fig. 18. The effect of a sensor failure on the level of observability.

Table 15
Different levels of partial link flow observability considering buffer sensors in the Fishbone network.

# of available sensors	Set of links equipped with buffer sensors	Avg. appearance of observed links equipped with buffer sensors	Avg. appearance of observed links equipped with available sensors	Level of observability (h value)
11	{1}	1	1.9	5
9	{2, 4, 6}	1.3	2	4
7	{2, 12, 14, 16, 18}	1.8	2	2

make it possible to employ the model to determine the location of available sensors. We employed the Fishbone network to show how the model can be employed for partial link flow observability. Table 15 presents the results of sensor location suggested by the model when, for simplicity purposes, all available sensors are assumed to be identical.

We used Eq. (17) to find the location of sensors, removing the binary variable y_{fj} and the parameter p_f from this equation as we assumed all sensors are identical. In the table, we considered different numbers of available sensors, all of which are less than the number of required sensors, i.e., 12 sensors, to reach full link flow observability. Table 15 also evaluates the average number of appearances of observed links instrumented with either available or buffer sensors in equations used for the link flow inference of unobserved links. According to this table, the average number of appearances of available sensors is always higher than the buffer sensors. In the last column of the table, the effect of available sensors on the level of observability, i.e., h, is studied. In this column, we considered the appearance of observed links equipped with buffer sensors in equations required for the link flow inference of unobserved links. If, among the observed links required for the link flow inference of an unobserved link, there is at least one observed link instrumented with buffer sensors, we considered that the flow of that unobserved link cannot be inferred. Comparing the first and the last column of Table 15, we see that the model attempts to minimize the effect of a decrease in available sensors on the level of observability. For instance, when there are three deficient sensors in the number of sensors required to reach full link flow observability in the Fishbone network (i.e., there are nine available sensors), the level of observability decreases to $h=4$, which means that the flow of only two unobserved links cannot be inferred, compared to the full link observability condition where $h=6$.

In Section 6 of this paper, we discussed the possibility of using the route flow information for evaluating the sensor deployments that lead to full link flow observability. A similar approach can be employed in the model to consider taking advantage of route flow information for the partial observability problem. This means that considering the available sensors and buffer sensors, the model should minimize the effect of available sensor failure on the link flow inference of unobserved links (first level optimization), while attempting to also minimize the effect of sensor failure on route flow information gain of independent routes, i.e., routes in $R^1 \cup R^2 \cup R^{3'}$. Although it is beyond the scope of this work, we believe that combining the problem of partial link flow observability, as well as route flow observability, into a single level optimization model, taking into account the failure of sensors, represents an interesting topic for future research.

11. Conclusion

The minimum set of sensor-equipped links for full link flow observability in a traffic network is not necessarily unique since a different set of observed links can lead to a different system of linear equations to be used for the link flow inference of unobserved links. With the possibility of sensor failure, different sets of observed links will result in different probabilities of inference loss of the unobserved links in a network. This paper investigates how the effect of sensor failure on the link flow inference of unobserved links can be considered in identifying the set of observed links in a traffic network. Two types of sensors (i.e., basic and advanced) with different failure probabilities were studied. Methodologically, we considered

two contributing factors in determining the location of sensors, namely the probability of missing the link flow inference of unobserved links due to the failure of sensors, as well as the effect of sensor failure on the link flow inference of unobserved links. These two factors are defined as the objective functions in the form of min-max and min-sum functions. We also combined these functions by considering the min-sum function as the objective function while setting a cap for the maximum value of the min-max function. We then proposed GA as a well-known heuristic to solve this problem. To generate the initial solution in the proposed GA, we suggested using the concept of new links to avoid the exhaustive search for constructing the sets of unobserved links. We applied the developed model for three numerical examples including the Fishbone, Sioux Falls, and Irvine networks. The results related to the Fishbone network indicated that the combined objective function formulation leads to better local optimal solutions compared to the situation when the min-sum and min-max functions are employed separately. We further explained how the effect of the above-mentioned factors can be cohesively addressed by minimizing the number of observed links required for the link flow inference of each unobserved link when the sensors are assumed to be identical. However, in the case of non-identical sensors, the installation of more advanced sensors is required to compensate for the larger number of observed links required for the link flow inference of that unobserved link. To take into consideration the fact that all links are not equally significant in a network, we also differentiated between major and minor roads to be instrumented with non-identical sensors in a traffic network. We suggested two different approaches to equip major and minor roads with sensors in reaching full link flow observability. The first was to manually equip links in the set of major roads with sensors while also studying the cases where the manually instrumented major links with sensors result in the matrix of unobserved links becoming a singular matrix. The second approach was to keep the constraints already applied to the identical sensors in place while updating the objective function to consider the major roads by incorporating the weights to signify the relative importance of major roads. The results of considering the major roads in identifying the location of sensors in the Sioux Falls network implied that the model attempts to assign more advanced sensors to major roads and to not include these roads in the set of unobserved links. As HVL can influence the failure rate of sensors, we also considered the effect of HVL on major and minor roads in determining the location of sensors in a network. The results of this assessment in the Sioux Falls network suggest that the model attempts both to install more advanced sensors on major roads traversed by a large number of heavy vehicles and to minimize the number of major links with high HVL in the set of unobserved links. The model achieved this goal without affecting the number of major roads with or without HVL in the set of observed links.

We studied the full link flow observability problem in the Irvine network to assess the applicability of the model in a large scale network. For this network, we compared the results obtained with the proposed model to those reported for one of the existing models in the literature, and showed the merit of the current model in handling large size networks as well as decreasing the impact of sensor failure on link flow inference of unobserved links.

The route flow information gain was another topic that we discussed in this work. After introducing different types of routes based on the mutual links traversed by these routes, we proposed a two-level optimization model that can evaluate different sensor layouts which can lead to full link flow observability and minimize the impact of sensor failure on link flow inference of unobserved links. The results related to the Fishbone network demonstrated that sensors failure in two different layouts, having similar sensor failure impact on link flow inference of unobserved links, can have dissimilar effects on route flow observability.

We investigated the location of redundant sensors, i.e. additional sensors which are not initially required for full link flow observability of a traffic network, but which can be installed in a network to maintain the link flow inference of unobserved links in the event of sensor failure. To find the location of redundant sensors, we considered all possible combinations of failure among sensors installed in links within a network. The results indicated that although considering all combinations of failure among sensors to determine the optimum location of redundant sensors is computationally expensive, there are a substantial number of combinations that prevent full link flow observability and therefore should not be considered in finding the location of redundant sensors.

In the final part of the study, we discussed the possibility of employing the proposed model for the partial link flow observability problem. After providing different definitions of partial link flow observability, we used the Fishbone network to show that the sensor positioning suggested by the proposed model attempts to minimize the chances of decrease in the level of link observability in a network. We also proposed the idea of buffer sensors to address the situation where the number of available sensors is not large enough to reach full link flow observability. The results of using buffer sensors for different numbers of sensors available in the Fishbone network demonstrated that the model attempts to install buffer sensors on links with the least number of appearances in equations needed for link flow inference of unobserved links. Further study can be carried out to extend the concept of sensor failure to the research of locating traffic detectors in traffic networks for OD estimation purposes.

Acknowledgments

This work is funded through Natural Sciences and Engineering Research Council of Canada (NSERC) (Grant No. RT735236) Discovery and Discovery Accelerator Supplement grants, an Alberta Motor Association - Alberta Innovates Technology Futures (AMA-AITF) (Grant No. 10002678) collaborative grant in Smart Multi-modal Transportation Systems and the Urban Alliance professorship in Transportation Systems Optimization. It is also jointly supported by research grants from the Research Committee of the Hong Kong Polytechnic University for the in-bound PhD student attachment program, and the

Research Grants Council of the Hong Kong Special Administrative Region, China (Project No. PolyU 152628/16E). The authors would like to thank both Dr. R. John Milne for his continued support and guidance as well as the anonymous reviewers for their insightful comments.

Appendix I

For identical sensors, if two layouts have the same average number of observed links required for the link flow inference of an unobserved link, i.e., having equal value of Y_3 introduced in Eq. (10), the expected number of unobserved links whose flow cannot be inferred due to the failure of sensors can be different, i.e., they have different values of Y_2 introduced in Eq. (9). An example of this scenario would be for instance, if there are two layouts A and B for a network, and the summation of non-zero values of the matrix $-T_u{}^{-1}T_o$ for each row of layouts A and B are similar except for rows j' and j'' in which:

$$\begin{cases} n^A_{j'} = n^B_{j'} + 1 \\ n^A_{j''} = n^B_{j''} - 1 \end{cases} \qquad n^A_{j''} \le n^A_{j'} \tag{I-1}$$

In Eq. (I-1), $n^A_{j'}$, $n^B_{j'}$ represent the summation of non-zero values of row j' in matrix $-T_u{}^{-1}T_o$ related to layouts A and B, respectively. These two layouts have the same value of Y_3 and the probability of missing the link flow inference is the same for all unobserved links except for the links j' and j''. If we subtract the Y_2 related to layout B, shown as $Y_2^{(B)}$, from the same value associate with layout A, shown as $Y_2^{(A)}$, then we reach the following equation:

$$\begin{aligned} Y_2^{(A)} - Y_2^{(B)} &= \left[\left(1-(1-p)^{n^A_{j'}}\right) + \left(1-(1-p)^{n^A_{j''}}\right)\right] - \left[\left(1-(1-p)^{n^B_{j'}}\right) + \left(1-(1-p)^{n^B_{j''}}\right)\right] \\ &= (1-p)^{n^B_{j'}} + (1-p)^{n^B_{j''}} - \left[(1-p)^{n^A_{j'}} + (1-p)^{n^A_{j''}}\right] \\ &\Rightarrow (1-p)^{n^A_{j'}+1} + (1-p)^{n^A_{j''}-1} - \left[(1-p)^{n^A_{j'}} + (1-p)^{n^A_{j''}}\right] = (1-p)^{n^A_{j'}}(-p) + (1-p)^{n^A_{j''}-1}(p) \\ &\Rightarrow (1-p)^{n^A_{j''}-1}\left[(1-p)^{n^A_{j'}-n^A_{j''}-1}(-p) + p\right] \ge 0 \end{aligned} \tag{I-2}$$

In Eq. (I-2), $(1-p)^{n^A_{j'}-n^A_{j''}-1}$ is a value between 0 and 1, and therefore the inequality in which $p(1-p)^{n^A_{j'}-n^A_{j''}-1} \le p$ is always valid and we can conclude that $Y_2^{(A)} \ge Y_2^{(B)}$. Therefore, layout B should be preferred over layout A as it has a lower value associated with expected number of unobserved links for which their flow cannot be inferred due to the failure of sensors, while both layouts have an identical average number of observed links required for the link flow inference of unobserved links.

Appendix II

In the Fishbone network, let's assume that the red highlighted links, including links 1, 2, 3, 4, 9, 10, 11, 12, 15, 16 and 18, are major roads in the network. According to the equation developed by Ng. (2012) and introduced in Section 2, 12 links in the Fishbone network should be equipped with sensors to reach full link flow observability. Therefore, the number of major roads is less than the number of links that should be instrumented with sensors, i.e., observed links. If we want to apply the manual approach introduced in Section 5.2 to equip the major roads with sensors, all major roads listed above should be considered as observed links, i.e., sensor-equipped links in this network and one of the links not included in the set of major roads should be instrumented with a sensor as well. In this case, among seven links, including links 5, 6, 7, 8, 13, 14, and 17, which are not in a set of major roads, six of them should be selected as the unobserved links. Knowing that links 13 and 14, 5 and 7, and 6 and 8 are three sets of bi-directional links which can create cyclic graphs in a directed network,[13] we need to select all links from at least two of these three sets to have six links as unobserved links in the Fishbone network. Therefore, unavoidably, the links selected to be in the set of unobserved links create the cyclic graph.[14] According to Bapat (2010), the column vectors of a matrix that create a cyclic graph are linearly dependent, and the matrix, while being a square matrix, is a singular one. In what follows, we provide a lemma and a proposition to indicate that the column vectors in the matrix of unobserved links should not induce a cyclic graph:

Fig. II-1

Lemma 1. *Let T be a $n \times m$ node-link incidence matrix that represents a network having m links and n non-centroid nodes. Any selections of column vectors of T are linearly independent if and only if the corresponding links of those selected columns don't induce a cyclic graph.*

[13] A network in which the links have directions.

[14] A cyclic graph or circular graph is a subset of links that construct a path known as a cycle such that the first node of the path corresponds to the last one (Pemmaraju and Skiena, 2003).

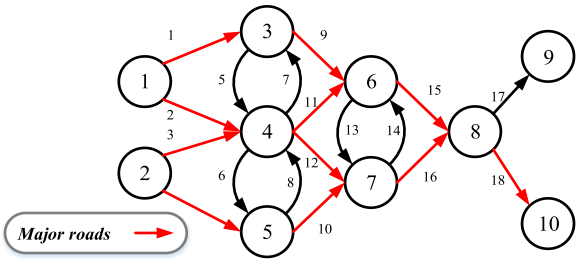

Fig. II-1. Consideration of major roads in the Fishbone network.

Proof. If k columns are selected from the matrix T, and p columns of the k columns,$p \leq k$, induce a cyclic graph, then Bapat (2010) proved that those p column vectors could be used to construct a matrix which is of the form $\begin{bmatrix} B \\ 0 \end{bmatrix}$, where B is the $p \times p$ matrix with column sums zero and represents the cyclic graph formed by the columns 1, ..., p. Therefore, B is singular[15] and the columns 1, ..., p are linearly dependent. This proof addresses the "only if" part of the Lemma 1. For the proof of the other part, please refer to Bapat (2010).

Based on the Lemma 1, further criteria should be met to assure the matrix of unobserved links, T_u, obtained from the set of new links is an invertible matrix:

Proposition 1. *The links selected from each set of new links to form the matrix of unobserved links T_u, should not induce a cyclic graph in order to be invertible.*

Proof. A square matrix that has linearly independent column vectors is invertible. Matrix T_u is a square matrix as already discussed by Xu et al. (2016). Moreover, based on the Lemma 1, the column vectors of T_u are linearly independent if they do not form a cyclic graph. Therefore, the square matrix T_u which has linearly independent column vectors can be inverted and used to infer the flow of unobserved links.

Appendix III

The following table presents the connected links and the sets of new links related to each non-centroid node in the Sioux Falls network. The table is borrowed from Table 5 in Xu et al. (2016).

Table III-1. The sets of new links associated with the non-centroid nodes in the Sioux Falls network

Non-centroid node	Connected links	New links
1	1,2,3,5	1,2,3,5
2	1,3,4,14	4,14
3	2,5,6,7,8,35	6,7,8,35
4	6,8,9,10,11,31	9,10,11,31
5	9,11,12,13,15,23	12,13,15,23
6	4,12,14,15,16,19	16,19
7	17,18,20,54	17,18,20,54
8	16,17,19,20,21,22,24,47	21,22,24,47
9	13,21,23,24,25,26	25,26
10	25,26,27,28,29,30,32,43,48,51	27,28,29,30,32,43,48,51
11	10,27,31,32,33,34,36,40	33,34,36,40
12	7,33,35,36,37,38	37,38
13	37,38,39,74	39,74
14	34,40,41,42,44,71	41,42,44,71
15	28,41,43,44,45,46,57,67	45,46,57,67
16	22,29,47,48,49,50,52,55	49,50,52,55
17	30,49,51,52,53,58	53,58
18	18,50,54,55,56,60	56,60
19	45,53,57,58,59,61	59,61
20	56,59,60,61,62,63,64,68	62,63,64,68
21	62,64,65,66,69,75	65,66,69,75
22	46,63,65,67,68,69,70,72	70,72
23	42,70,71,72,73,76	73,76
24	39,66,74,75	–

[15] The determinant if this matrix is zero and therefore is not invertible.

References

Bapat, R.B., 2010. Graphs and Matrices. Springer, New York.

Bianco, L., Confessore, G., Reverberi, P., 2001. A network based model for traffic sensor location with implications on O/D matrix estimates. Transport. Sci. 35 (1), 50–60.

Bianco, L., Confessore, G., Gentili, M., 2006. Combinatorial aspects of the sensor location problem. Ann. Oper. Res. 144 (1), 201–234.

Bianco, L., Cerrone, C., Cerulli, R., Gentili, M., 2014. Locating sensors to observe network arc flows: exact and heuristic approaches. Comput. Oper. Res. 46, 12–22.

Castillo, E., Conejo, A.J., Menéndez, J.M., Jiménez, P., 2008a. The observability problem in traffic network models. Comput. Aided Civil Infrastruct. Eng. 23 (3), 208–222.

Castillo, E., Jimenez, P., Menéndez, J.M., Conejo, A.J., 2008b. The observability problem in traffic models: algebraic and topological methods. IEEE Trans. Intell. Transport. Syst. 9 (2), 275–287.

Castillo, E., Gallego, I., Sanchez-Cambronero, S., Rivas, A., 2010. Matrix tools for general observability analysis in traffic networks. IEEE Trans. Intell. Transport. Syst. 11 (4), 799–813.

Castillo, E., Gallego, I., Menéndez, J.M., Jiménez, P., 2011. Link flow estimation in traffic networks on the basis of link flow observations. J. Intell. Transport. Syst. 15 (4), 205–222.

Castillo, E., Nogal, M., Rivas, A., Sánchez-Cambronero, S., 2013. Observability of traffic networks. Optimal location of counting and scanning devices. Transportmetrica B 1 (1), 68–102.

Castillo, E., Calviño, A., Lo, H.K., Menéndez, J.M., Grande, Z., 2014. Non-planar hole-generated networks and link flow observability based on link counters. Transport. Res. Part B 68, 239–261.

Chen, A., Pravinvongvuth, S., Chootinan, P., Lee, M., Recker, W., 2007. Strategies for selecting additional traffic counts for improving OD trip table estimation. Transportmetrica 3 (3), 191–211.

Chen, A., Chootinan, P., Recker, W., 2009. Norm approximation method for handling traffic count inconsistencies in path flow estimator. Transport. Res. Part B 43 (8-9), 852–872.

Chootinan, P., Chen, A., Yang, H., 2005. A bi-objective traffic counting location problem for origin-destination trip table estimation. Transportmetrica 1 (1), 65–80.

Chootinan, P., Chen, A., 2011. Confidence interval estimation for path flow estimator. Transport. Res. Part B 45 (10), 1680–1698.

Danczyk, A., Di, X., Liu, H.X., 2016. A probabilistic optimization model for allocating freeway sensors. Transport. Res. Part C 67, 378–398.

Ehlert, A., Bell, M.G., Grosso, S., 2006. The optimisation of traffic count locations in road networks. Transport. Res. Part B 40 (6), 460–479.

Federal Highway Administration, 2006. Traffic Detector Handbook: Third Edition—Volume II. Turner-Fairbank Highway Research Center, McLean, VA Publication FHWA- HRT-06-139.

Fei, X., Mahmassani, H., Eisenman, S., 2007. Sensor coverage and location for real-time traffic prediction in large-scale networks. Transport. Res. Rec. 2039, 1–15.

Fei, X., Mahmassani, H.S., Murray-Tuite, P., 2013. Vehicular network sensor placement optimization under uncertainty. Transport. Res. Part C 29, 14–31.

Fei, X., Mahmassani, H.S., 2011. Structural analysis of near-optimal sensor locations for a stochastic large-scale network. Transport. Res. Part C 19 (3), 440–453.

Fu, C., Zhu, N., Ling, S., Ma, S., Huang, Y., 2016. Heterogeneous sensor location model for path reconstruction. Transport. Res. Part B 91, 77–97.

Fu, C., Zhu, N., Ma, S., 2017. A stochastic program approach for path reconstruction oriented sensor location model. Transport. Res. Part B 102, 210–237.

Gentili, M., Mirchandani, P.B., 2012. Locating sensors on traffic networks: models, challenges and research opportunities. Transport. Res. Part C 24, 227–255.

Gentili, M., Mirchandani, P.B., 2018. Review of optimal sensor location models for travel time estimation. Transport. Res. Part C 90, 74–96.

Gillespie, T.D., 1993. Effects of Heavy-Vehicle Characteristics on Pavement Response and Performance. National Academy Press, Washington, D.C. United States Transportation Research Board.

Guan, J., Aral, M.M., 1999. Progressive genetic algorithm for solution of optimization problems with nonlinear equality and inequality constraints. Appl. Math. Modell. 23 (4), 329–343.

Hadavi, M., Shafahi, Y., 2016. Vehicle identification sensor models for origin–destination estimation. Transport. Res. Part B 89, 82–106.

Hallenbeck, M.E., Selezneva, O.I., Quinley, R., 2014. Verification, Refinement, and Applicability of Long-Term Pavement Performance Vehicle Classification Rules (No. FHWA-HRT-13-091). Federal Highway Administration. Office of Infrastructure Research and Development, United States.

He, S.X., 2013. A graphical approach to identify sensor locations for link flow inference. Transport. Res. Part B 51, 65–76.

Hu, S.R., Peeta, S., Chu, C.H., 2009. Identification of vehicle sensor locations for link-based network traffic applications. Transport. Res. Part B 43 (8), 873–894.

Klein, L.A., Mills, M.K., Gibson, D., Klein, L.A., 2006. Traffic Detector Handbook: Volume II (No. FHWA-HRT-06-139). Federal Highway Administration, United States.

Li, X., Ouyang, Y., 2011. Reliable sensor deployment for network traffic surveillance. Transport. Res. Part B 45 (1), 218–231.

Mínguez, R., Sánchez-Cambronero, S., Castillo, E., Jiménez, P., 2010. Optimal traffic plate scanning location for OD trip matrix and route estimation in road networks. Transport. Res. Part B 44 (2), 282–298.

Morrison, D.R., Martonosi, S.E., 2015. Characteristics of optimal solutions to the sensor location problem. Ann. Oper. Res. 226 (1), 463–478.

Ng, M., 2012. Synergistic sensor location for link flow inference without path enumeration: a node-based approach. Transport. Res. Part B 46 (6), 781–788.

Ng, M., 2013. Partial link flow observability in the presence of initial sensors: solution without path enumeration. Transport. Res. Part B 51, 62–66.

Pemmaraju, S., Skiena, S., 2003. Computational Discrete Mathematics: Combinatorics and Graph Theory With Mathematica®. Cambridge university press.

Rinaldi, M., Viti, F., 2017. Exact and approximate route set generation for resilient partial observability in sensor location problems. Transport. Res. Part B 105, 86–119.

Schrank, D., Eisele, B., Lomax, T., Bak, J., 2015. 2015 Urban Mobility Scorecard. Texas A&M Transportation Institute, Texas, United States.

Viti, F., Rinaldi, M., Corman, F., Tampère, C.M., 2014. Assessing partial observability in network sensor location problems. Transport. Res. Part B 70, 65–89.

Wang, N., Gentili, M., Mirchandani, P., 2012. Model to locate sensors for estimation of static origin-destination volumes given prior flow information. Transport. Res. Rec. 2283, 67–73.

Wang, N., Mirchandani, P., 2013. Sensor location model to optimize origin-destination estimation with a bayesian statistical procedure. Transport. Res. Rec. 2334, 29–39.

Xu, X., Lo, H.K., Chen, A., Castillo, E., 2016. Robust network sensor location for complete link flow observability under uncertainty. Transport. Res. Part B 88, 1–20.

Yang, H., H. Bell, M.G., 1998. Models and algorithms for road network design: a review and some new developments. Transport Rev. 18 (3), 257–278.

Zhan, F., Wan, X., Cheng, Y., Ran, B., 2018. Methods for multi-type sensor allocations along a freeway corridor. IEEE Intell. Transport. Syst. Mag. 10 (2), 134–149.

Zhou, X., List, G.F., 2010. An information-theoretic sensor location model for traffic origin-destination demand estimation applications. Transport. Sci. 44 (2), 254–273.

Zhu, N., Ma, S., Zheng, L., 2017. Travel time estimation oriented freeway sensor placement problem considering sensor failure. J. Intell. Transport. Syst. 21 (1), 26–40.